REPORT DOCUMENTATION PAGE

AFRL-SR-AR-TR-03-

0412

1. AGENCY USE ONLY *(Leave blank)*	2. REPORT DATE	3. REPORT T
	1 OCT 03	FINAL REPORT 1 AUG 00 TO 30 APR 02

4. TITLE AND SUBTITLE
HIGH ENERGY DENSITY MATERIALS

5. FUNDING NUMBERS

F49620-00-C-0033

6. AUTHOR(S)
PROESSOR DAVID BOMBERGER

G6110/09

63765E

7. PERFORMING ORGANIZATION NAME(S) AND ADDRESS(ES)
SRI INTERNATIONAL
333 RAVENSWOOD AVENUE
MENLO PARK, CA 94025-3493

8. PERFORMING ORGANIZATION REPORT NUMBER

9. SPONSORING/MONITORING AGENCY NAME(S) AND ADDRESS(ES)

AFOSR/NL
4015 WILSON BLVD, RM 713
ARLINGTON, VA 22203-1954

10. SPONSORING/MONITORING AGENCY REPORT NUMBER

11. SUPPLEMENTARY NOTES

12a. DISTRIBUTION AVAILABILITY STATEMENT

APPROVE FOR PUBLIC RELEASE: DISTRIBUTION UNLIMITED.

12b. DISTRIBUTION CODE

13. ABSTRACT *(Maximum 200 words)*
Synthetic pathways to the nitroazoxyamine, pentazole-N-oxide, and triazanitrate anions have been explored at a fundamental level. The reaction of nitrene equivalents such as organic azides, N-haloamines, N-acyl hydroxylamines, N,O-diacyl hydroxylamines, and amides in the presence of lead tetra-acetate or phenyliodine diacetate, acting on N,N dialkylnitrosoamines in an attempt to generate alkylazoxyamines have all been examined. Initial results were not encouraging; in response to this, the N,N-dialkylnitrosoamine was silylated, methylated, and acylated to give 1,1-dialkyl-2silyloxy diazenium cation and its analogues. These cations were reacted with a wide array of nucleophillic nitrene equivalents such as fluoronitramide anion or monobromo-tert, butylamine; again, no azoxy amine was observed. Intramolecular versions of the above mentioned methodologies were contrived; the appropriate intermediates were synthesized, characterized, and subjected to a variety of conditions designed to effect the intramolecular synthesis of the alkylazoxyamine, a useful precursor to the heretofore unknown nitroazoxyamine (diazanitrate). Still, no obvious evolution of the desired azoxyamine was observed. Many variations remain to be explored. One clear success in this program was the invention of HYDROXYNITROUREA, a high density oxidizer with potential use as a replacement for perchlorate. Kilogram quantities were made and tested commerciallly; it tended to burn too fast at elevated pressures. The ammonium salt of HNU shows much promise as a burn rate attenuator, and this is presently being explored.

14. SUBJECT TERMS

15. NUMBER OF PAGES

16. PRICE CODE

17. SECURITY CLASSIFICATION OF REPORT	18. SECURITY CLASSIFICATION OF THIS PAGE	19. SECURITY CLASSIFICATION OF ABSTRACT	20. LIMITATION OF ABSTRACT
UNCLAS	UNCLAS	UNCLAS	

SRI International

F49620-00-C-0033

HIGH ENERGY DENSITY MATERIALS

SRI Project P10926
For the Period August 30, 2000 through January 30, 2002

Prepared by:

Jeffrey C. Bottaro
Mark Petrie
Paul E. Penwell
Allen L. Dodge
Chemical Science and Technology Laboratory

Prepared for;

Air Force Office of Scientific Research
4015 Wilson Boulevard
Room 713
Arlington, VA 22203-1954

Attention: Wendy M. Veon
           Administrative Contracting Officer

Approved:

Robert B. Wilson Jr.
Director
Chemical Science and Technology Laboratory
Physical Sciences Division

20031028 195

CONTENTS

BACKGROUND

The search for superior energetic materials as explosives, propellants, gas generators, and pyrotechnics is a multinational endeavor that has been underway for several decades; in fact, the earliest efforts in this area extend all the way back into the middle of the nineteenth century with the discoveries of nitroglycerine and TNT.

The definition of what constitutes a superior energetic material is heavily dependent upon the application involved; each application has its own select set of relevant criteria. Thus, explosive performance is equated with detonation velocity and pressure, while rocket propellant performance is equated with specific impulse, a multiparameter function incorporating temperature, pressure, and molecular weight of the exhaust gasses. It is, therefore, unlikely that any single material will excel at all possible applications, especially when one adds safety requirements to the already complex set of performance requirements.

One critical deficiency in preexisting energetic materials technology is the relative lack of high-valency, high nitrogen functional groups, which will, in theory enable the synthesis of three-dimensional cage compounds possessing unprecedented energy and density. The fact that diamond has a density of 3.5 g/cc is a strong indicator that a highly elaborate cage structure, enabled exclusively by high valency functional groups is a prerequisite to the attainment of densities over 2.0 g/cc, which is the present benchmark for state-of-the-art energetic materials.

Our first consideration was thus the conception of a library of unprecedented, energetic, high-valency, high nitrogen functional groups whose bond orders and other electronic attributes made them realistic, attainable targets. A list of these new functional groups is shown in Table 1.

The diazanitrate, shown first in Table 1, is formally the adduct of a nitrene and a nitrosamine (see Figure 1). Our preliminary efforts toward this goal entailed all possible variants of this strategy and we attempted a variety of novel approaches to this end.

1
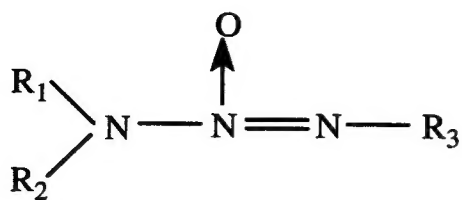
DIAZANITRATE (Trivalent)
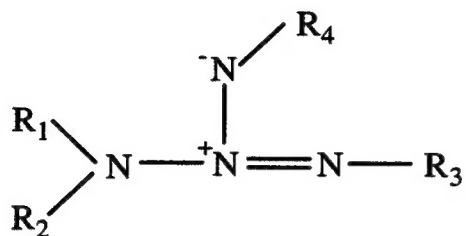
TRIAZANITRATE (Tetravalent)
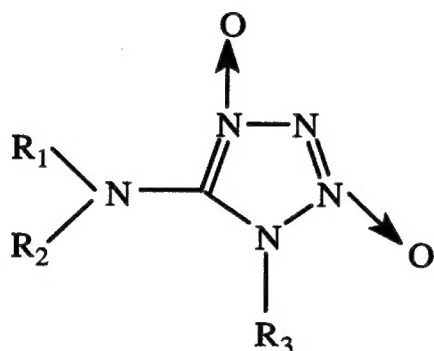
AMINOTETRAZOLE
DIOXIDE   (Trivalent)
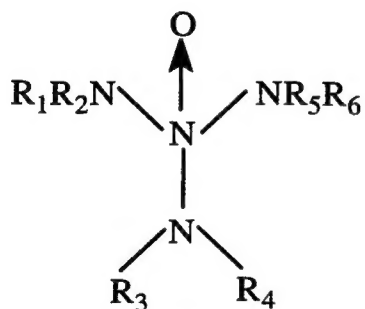
TRIAMINO
AMINE OXIDE (Hexavalent)

Table 1. High valency energetic groups.

2
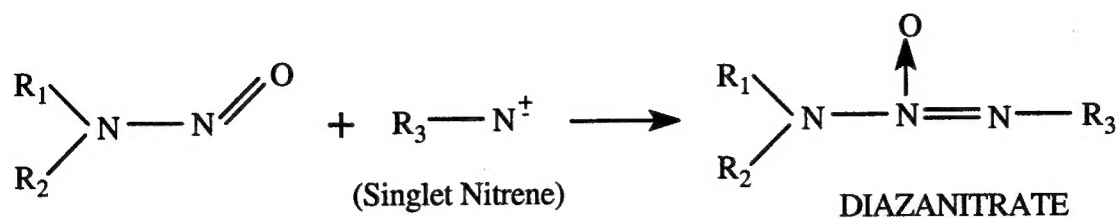
Figure 1

DIALKYL NITROSAMINES REACTING WITH T-BUTYL MONO-N-BROMO AMINE AND T-BUTYL-N,N-DIBROMOAMINE

This was the technique utilized by the Russians at the Zelinskii Institute to elaborate nitroso-aromatics to the corresponding t-butyl azoxyaromatics. These materials were easily nitrated to the corresponding nitroazoxy aromatics (Figure 2).
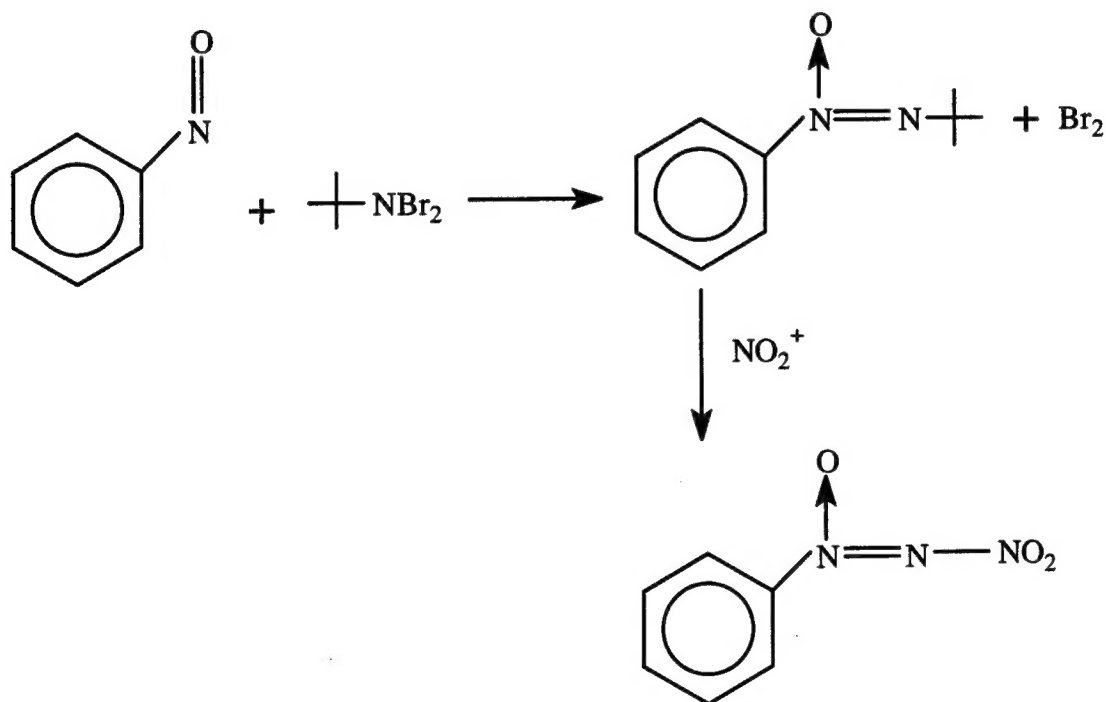
Figure 2. Russian synthesis of nitroazoxyaromatics.

3

Extensive effort was made to add nitrenes or nitrene equivalents to the N,N' dialkyl nitrosamine as shown in figure 1. N-lithio-O-alkyl hydroxylamines (shown in Figure 3) are potential nitrene equivalents in that they can conceivably add to nitrosamines, with ultimate loss of alkoxide lithium salt (Figure 4)

$$R\text{---}N\text{---}O\text{---}R'$$
$$\underset{\displaystyle Li}{|}$$
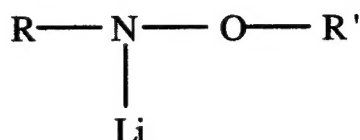
Figure 3. N-lithio-O-alkyl hydroxylamines.
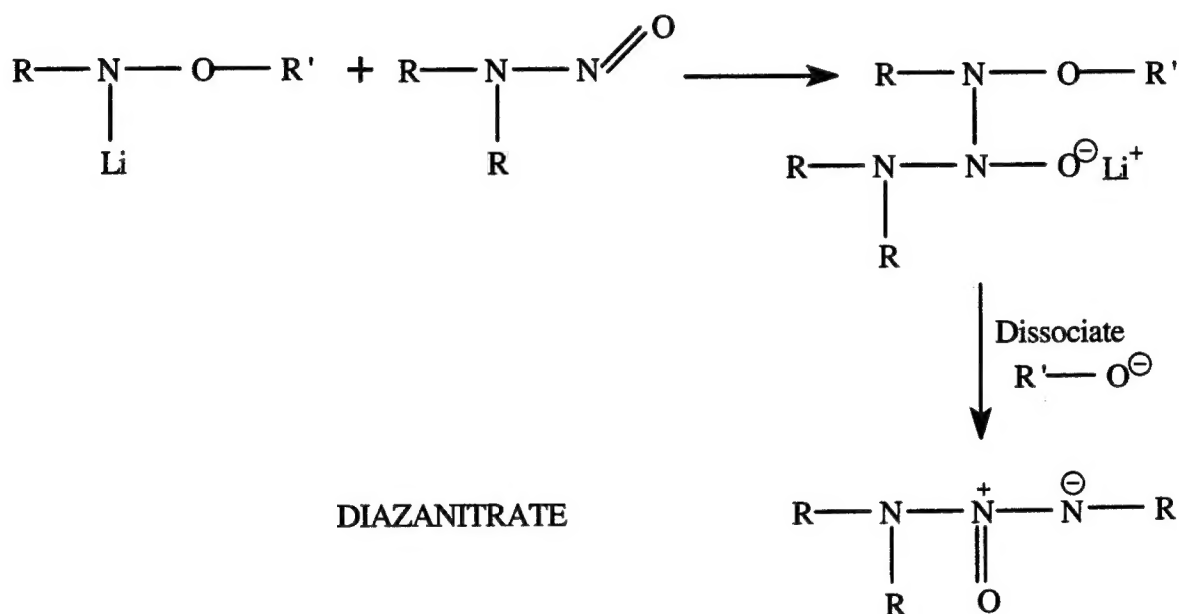
Figure 4. Use of N-lithio hydroxylamines as basic nitrene equivalents in the diazanitrate synthesis.

The principal lesson derived from this work is that the dialkyl nitrosamine is far less reactive toward both nucleophillic and electrophillic reagents than is the nitroso aromatic. Although this was anticipated at the outset, the magnitude of the reactivity differential between the nitroso aromatics observed by the Russians and the nitrosamines observed by our group was surprising. A wide range of nitrene equivalents was reacted with N,N dimethyl nitrosamine (Caution: Toxic—dispose of all reaction mixtures by solvolysis in H_2SO_4!) with no positive results. These are shown in Table 2.

Table 2. Nitrene equivalents used in attempted reaction with N,N-dimethylnitrosamine.

1. Tert.-butyl azide/CuCl/Rh[i] acetate

2. Diethoxyphosphoryl azide/CuCl/RH[i] acetate

3. N,O diacetyl hydroxylamine lithium salt

4. N,O dimethyl hydroxulamine lithium salt

5. N-Bromo-t-butylamine/CuCl/Rh[i] acetate

6. N-chloro-N-sodio-benzene sulfonamide

ALTERNATIVE STRATEGY FOR SYNTHESIS OF THE DIAZANITRATE FUNCTION

To circumvent the difficulties encountered in the addition of nitrene equivalents to dimethyl nitrosamine, other approaches were tried. One involved perturbation of the electron density of the nitroso group by placing it in proximity of other electron-withdrawing groups, which are removable under mild conditions. One such group examined was the N-methyl-N-nitroso alkyl carbamate (Figure 5).
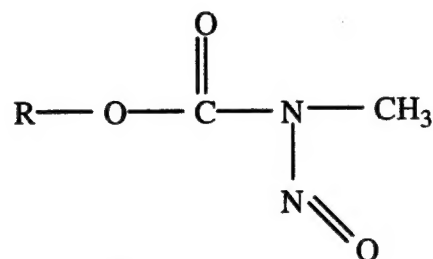
Figure 5. N-nitroso-N-methyl alkyl carbamate.

This is easily prepared by reacting methyl isocyanate with methyl alcohol, followed by N_2O_3 or nitrous acid. These materials suffered some of the same problems experienced with the simple dialkyl nitrosamines; in addition, they tended to decompose on standing at room temperature. We further explored the possibility of adding lithium salts of amines to the N-nitroso-N'-alkyl-N" alkyl hydroxylamines with the intention of clearing the alkoxide and deriving the desired diazanitrate (Figure 6).
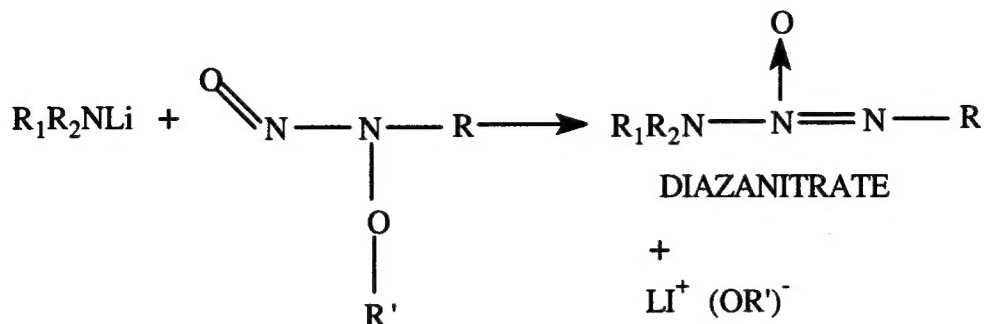
Figure 6. N-nitroso-N-alkyl-N'-alkyl hydroxylamines reaction with N-lithio secondary amines.

Unfortunately, this tactic resulted in the formation of multiple unstable products which could not be readily characterized. This surprised as considerably, as nitrosamines are known to be electrophillic toward N-lithiated amines. Frustrated by attempts at the synthesis of the diazanitrate function by methodologies involving the use of a nitrosamine intermediate, we began to explore methodologies involving the assembly of the diazanitrate by way of exchange of nitrogen for oxygen in the dinitramide anion or any of a number of its covalent derivatives (Figure 7).
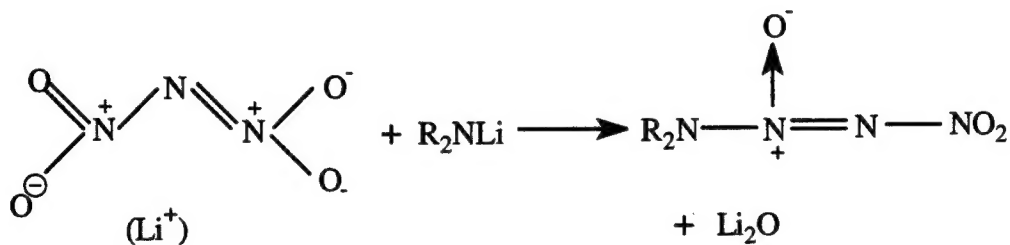
Figure 7. Synthesis of diazanitrate framework (as a mono-nitro derivative) by reaction of lithium dinitramidte with an N-lithiated amine.

In this instance, N-lithio-tert.butyl amine was reacted with anhydrous lithium dinitramide. Only one product was obtained in 50% yield when the reaction was run at –78°C in tetra-hydrofuran, warming to room temperature with a careful buffered acidic workup: N-(tertiary butyl) nitramine (Figure 8).

$$\text{—} \overset{|}{\underset{|}{}} \text{NH Li} + \text{Li}^+ \text{ N}_3\text{O}_4^- \longrightarrow \text{—} \overset{|}{\underset{|}{}} \text{NHNO}_2$$

(+ uncharacterized
inorganic by-product)
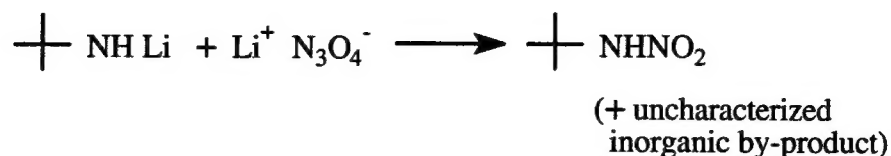
Figure 8. Reaction of lithium tert.-butylamide with lithium dinitramide.

Only the smallest amount of gassing was observed. As a result of this, other versions of this methodology were explored in the hope of realizing this elusive methodology of using dinitramides as nitroazoxy transfer agents to give, ultimately, the desired diazanitrate in the form of an N-(nitroazoxy) amine or its anionic form. One such approach involved the reaction of N-(trialkyl-silyl amines with O-trialkylsilyl dinitramide under catalysis by trimethylsilyl trifluoromethane-sulfonate (Figure 9).

$$\text{R}_2\text{N} \text{—} \text{SiMe}_3 + \text{Me}_3\text{Si} \text{—} \text{O} \text{—} \overset{\overset{O}{\uparrow}}{\text{N}} \text{=\!=} \text{N} \text{—} \text{NO}_2$$

$$\Big\downarrow \quad \text{Me}_3\text{Si} \text{—} \text{O} \text{—} \text{SO}_2\text{CF}_3 \quad \text{catalyst}$$

$$\text{R}_2\text{N} \text{—} \overset{\overset{O}{\uparrow}}{\text{N}} \text{=\!=} \text{N} \text{—} \text{NO}_2$$
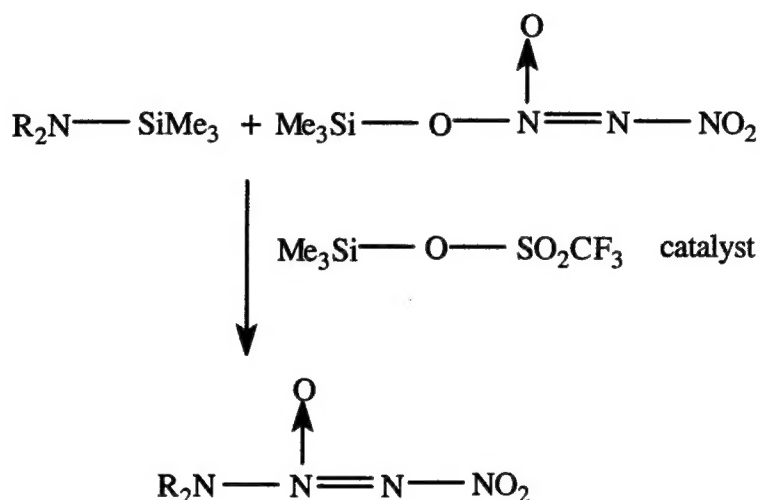
Figure 9. Attempted synthesis of diazanitrate in the form of an N-(nitrosoxy)amine
by way of acid catalysis.

To ensure that the catalyst and the silylated amine were compatible, samples of these materials were mixed and no heat evolution was observed nor was there a phase-change.

HYDROXYNITROUREA (HNU)

The one clear cut success in this endeavor was the discovery and scaleup of hydroxynitrourea shown in Figure 10.

$$H—O—N—C—N—NO_2$$
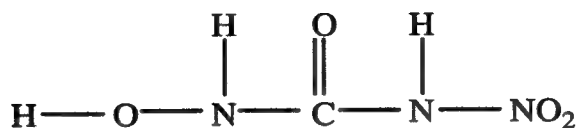
Figure 10. Hydroxynitrourea.

The decision to pursue this synthesis was driven by its simplicity, its high oxidation state, and the obvious fact that it should burn clean due to the complete absence of any carbon-carbon bonds, which are usually required for soot-formation. The synthesis of HNU succeeded on its first attempt and scaleup to 1/2 kilogram was reasonably straightforward. The synthesis is shown in Figure 11.

$$Na^+ \quad O_2N—\bar{N}—C—O—Et \quad + \quad NH_2OH \quad + \quad NaOH$$

$$Na^+ \quad O_2N—\bar{N}—C—N—\bar{O}$$

$$H_2SO_4$$

$$H—O—N—C—N—NO_2 \quad + \quad Na_2SO_4 \qquad ppt$$

short SiO$_2$ column

pure crystalline HNU

Figure 11. HNU synthesis.

8

SALTS OF HNU

The salts of HNU were well-behaved. The ammonium salt (see Appendices), prepared trivially by reaction of HNU with ammonia in methanol, has no apparent hygroscopicity and a decomposition temperature of 155°C. The hydrazinium and hydroxyl-ammonium salts were somewhat hygroscopic and pose formulation problems as a result. The rapid burning of HNU in preliminary small motor and strand studies may be attenuated by adding ammonium HNU to the formulation; this may result in cooler burning with trapping of some nitrogen oxides in the combustion process.

ATTENUATED DEHYDRATIVE CYCLIZATION OF HYDROXYNITROUREA

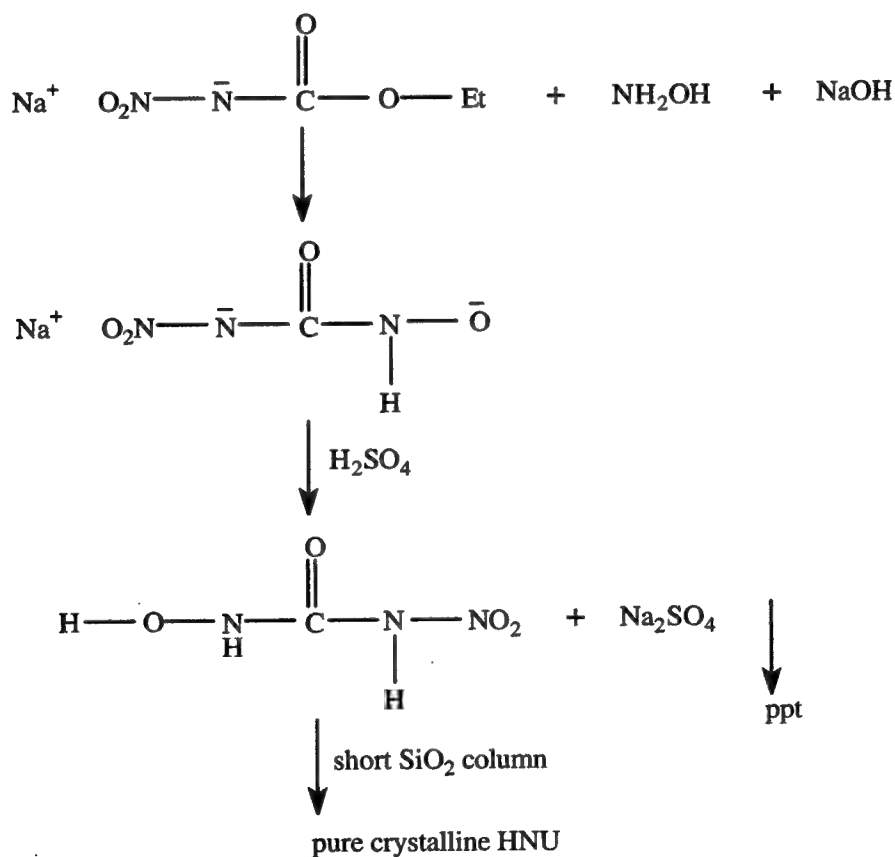Due to the undesirable acidity of HNU, an attempt was made to dehydratively cyclize it, to give a neutral species, which might also enjoy high density (see Figure 12).
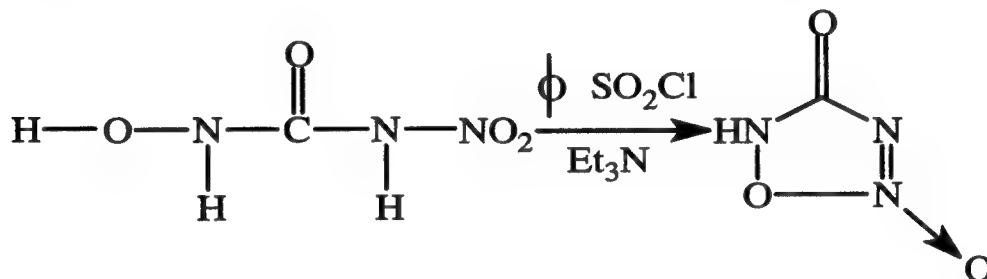
Figure 12. Dehydrative cyclization of HNU.

Unfortunately, all variants on the benzenesulfonyl chloride/triethylamine dehydration failed, giving only gas and a vigorous exotherm. Dicyclohexyl carbodiimide, phenyl isocyanate, $POCl_3$ with Et_3N all behaved in this manner, in spite of the fact that there is no apparent design flow in the product shown. It is without strain, it is aromatic, and has one hydrogen-bond

The synthesis of HNU was sensitive to counter ion and conditions. The use of potassium hydroxide rather than sodium hydroxide resulted in intractable polyphasic gels which could neither be centrifuged nor filtered.

The properties of hydroxynitrourea were impressive and are displayed in Table 2.

Table 2. Properties of HNU

Heat of formation[1]	-60.88 kcal per mole
Impact sensitivity	half that of RDX
DSC[2]	decomposes at 145°C
Hygroscopicity	nonexistent at <90% relative humidity
Density	1.91 g/cc[3]
ABL Friction[1]	50 @ 8
ESD (J) confined	4
ESD (unconfined)	≥ 8
TC friction	19.5 in.
SBAT	193°F

1. Courtesy of Tom Highsmith and coworkers at Morton Thiokol
2. See Appendix
3. Courtesy of Richard Gilardi and coworkers at NRL

Preliminary studies of burn rate of HNU were not encouraging; optimization of pressure exponents awaits formulation studies.

Inspired by the synthesis and properties of HNU, we set out to synthesize hydroxy nitroguanidine. The synthesis is shown in Figure 13.

The synthesis was successful, but the properties were less than ideal. The thermal stability was unacceptable with decomposition occurring at barely more than 100°C. This family of compounds was thus abandoned.

INTRAMOLECULAR TEMPLATES FOR DIAZANITRATE SYNTHESIS

To enhance the probability of successful addition of nitrene or nitrene equivalent to an N,N dialkyl nitrosamine, a series of intramolecular templates based on Figure 14 were synthesized and subjected to reaction conditions appropriate for the generation of a nitrene or nitrene equivalent. These materials, unfortunately, did not react cleanly and gave unstable, poorly characterizable products.
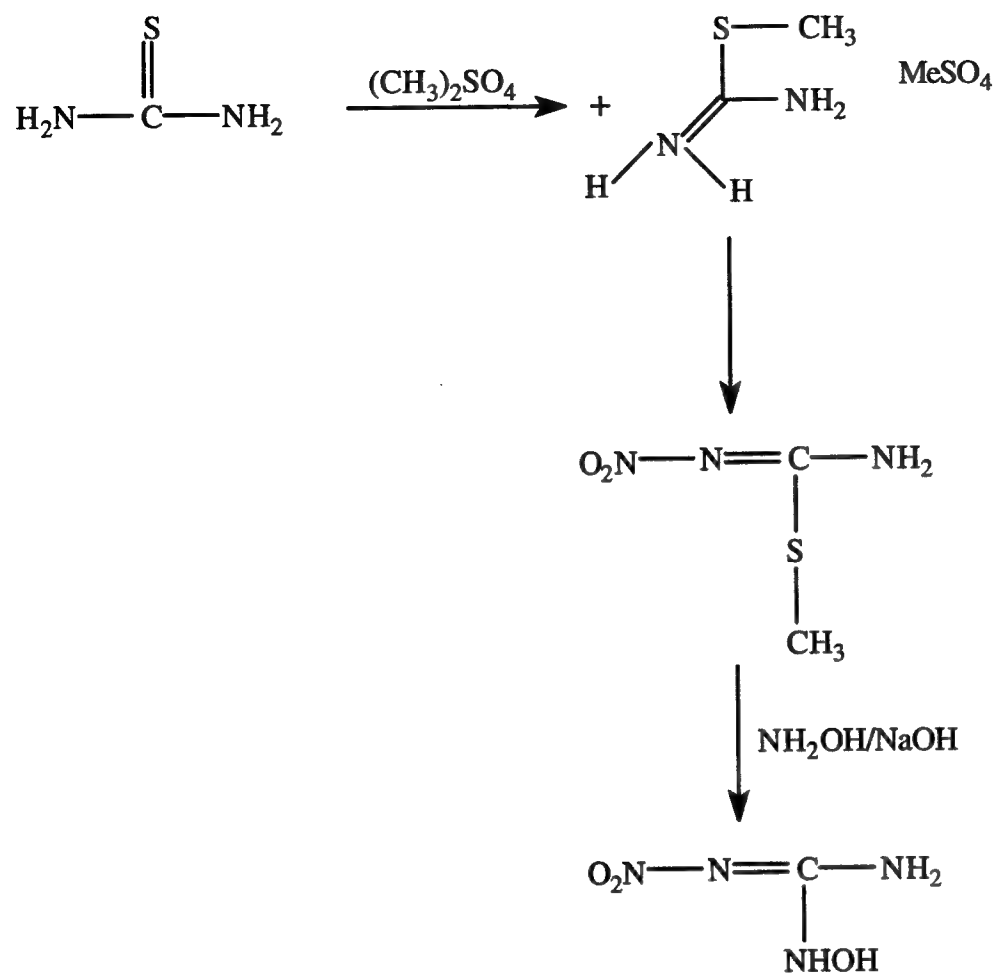
Figure 13. Hydroxynitroguanidine synthesis.

X,Y = H,N
H,OH
N = N = 3
Br,Br
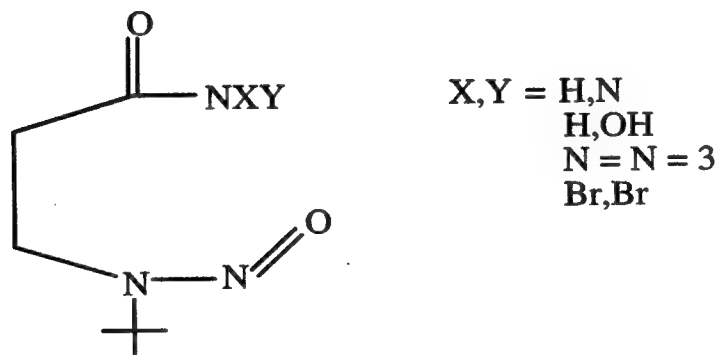
Figure 14. Diazanitrate synthesis templates.

These materials were all synthesized by beta-addition of tert-butylamine to methyl acrylate or acrylamide, followed by nitrosation of the resulting secondary amine with n-butyl nitrite. The x-ray structures are shown in the Appendix, and confirm the structures. In the case of the X,Y = H,H adduct shown in Figure 15, the amide was subjected to oxidation by bromine in aqueous base, phenyl iodine diacetate, lead tetra-acetate, permanganate, chromium trioxide, and copper II acetate. In no case could the cyclic triazine 2-oxide (Figure 16) be isolated and characterized conclusively.
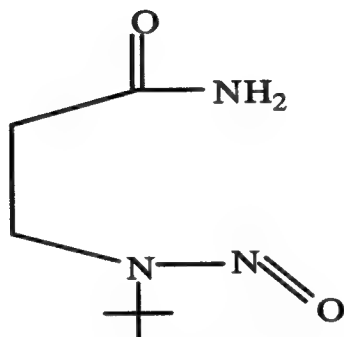
Figure 15. Beta-nitrosamine acrylamide.
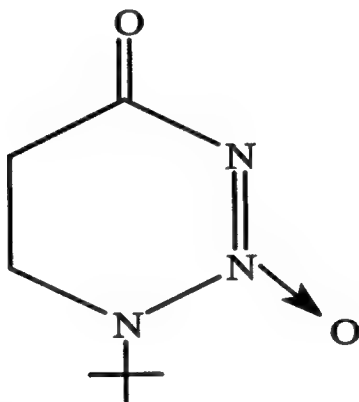
Figure 16. Desired diazanitrate adduct.

In another variant of the intramolecular addition of nitrene to nitrosamine, N-(beta azido ethyl)-N-(tert-butyl)nitrosamine whose structure and synthesis are shown in Figure 17 was subjected to a regime of azide degradation reactions reminiscent of the previous intramolecular scheme leading to a six-membered diazanitrate.
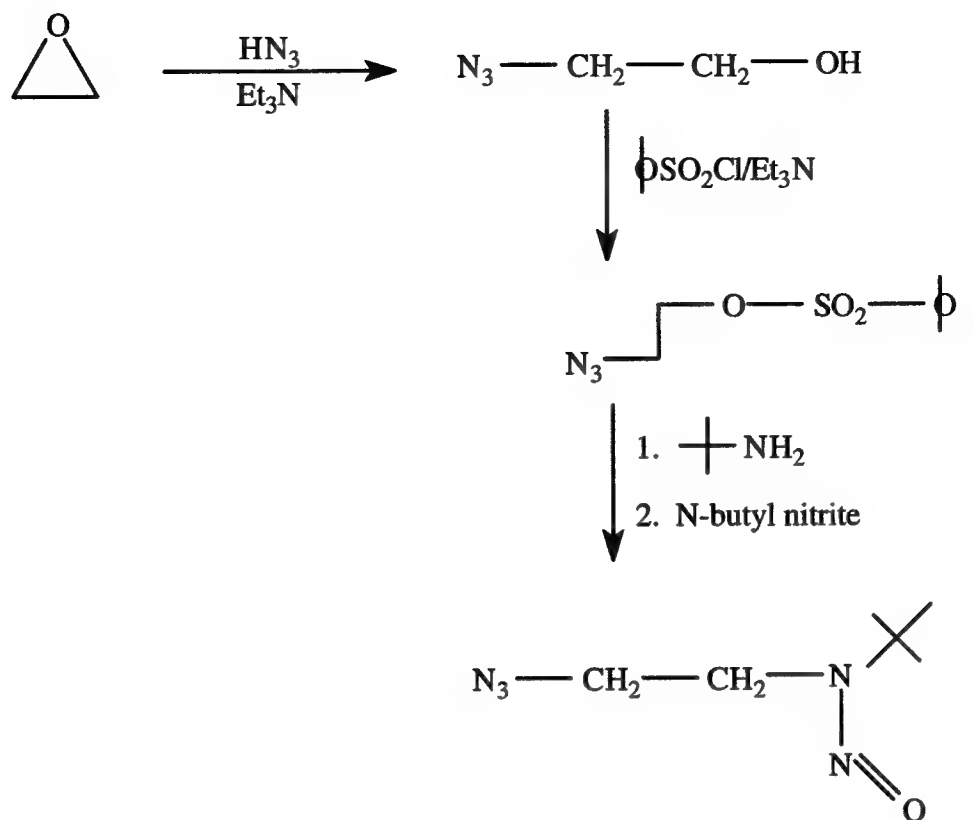
Figure 17. Synthesis of beta(azido ethyl)-N-(tert-butyl)nitrosamine.

Thus, this material was subjected to heat, catalysts, and even Lewis acid catalysts in an attempt to realize the diazanitrate analogue shown in Figure 18, which was observed.
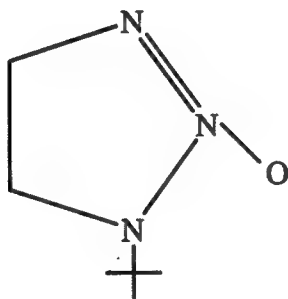
Figure 18. Diazanitrate analogue anticipated from the degradation of beta-(azido ethyl)-N-(tert-butyl)nitrosamine.

REACTION OF NITROSAMINES AND NITROSO AROMATICS WITH NITRENE AND CARBENE PRECURSORS: ATTEMPTS AT NITRO NITRONES, NITROAZOXY, AND FLUOROAZOXY DERIVATIVES

Combining N-nitroso-3,3'-dinitroazetidine with trinitromethanide, dinitromethanide, or dinitrocyanomethanide in acetonitrile gave no observable reaction by TLC, as shown in Figure 19.

$$(X = -NO_2, -H, -CN)$$
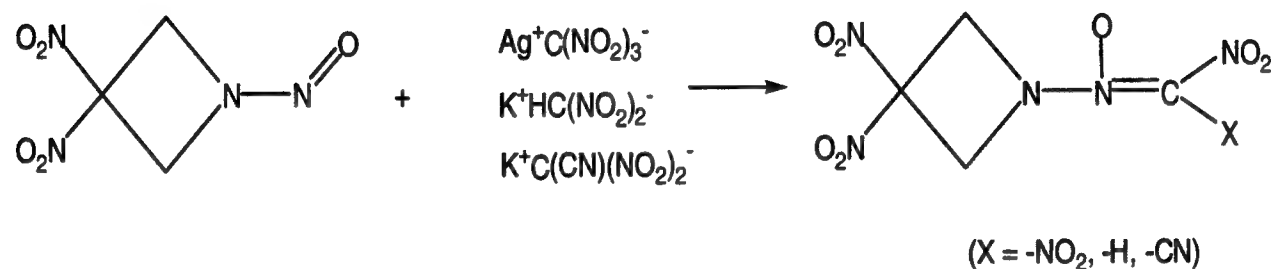
Figure 19. Reaction of N-nitroso-3,3-dinitroazetidine with carbene and nitrene precursors.

When nitroso aromatics are reacted with carbene and nitrene precursors, azoxy and nitrene products are known to form (Figure 20).

$$(Y = -H, -NMe_2, -NO_2)$$

$$(X = -NO_2, -H, -CN)$$
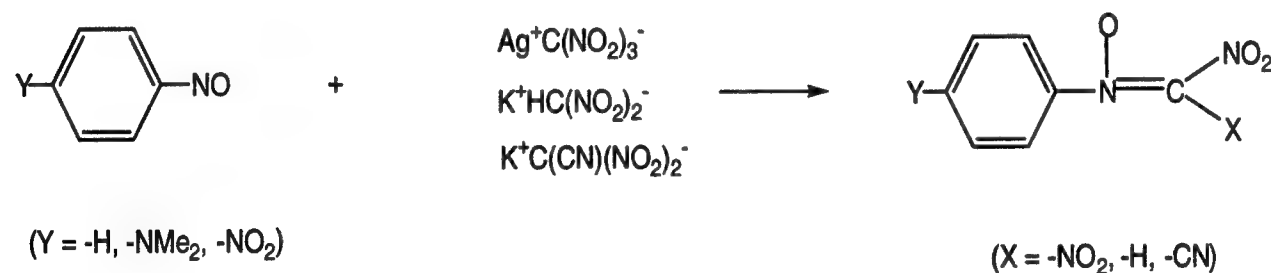
Figure 20. Reaction of nitroso aromatics with carbene and nitrene precursors.

Various combinations of the 3x3 matrix gave an observable reaction in most cases. Invariably these reactions lead to a myriad of products. Identification of the products is on-going.

There is precedent in the literature for the reaction of HNF2 or N2F4 with nitroso species (Figure 21) to give the fluroazoxy functional group. Similarly, reaction of a nitroso group with t-butyl and adamantyl difluoroamines may generate difluoroamine to give fluoroazoxy by way of a "fluoronitrene." The difluoroamino starting materials have been generated in situ by Selectfluor fluorination of the amines. Reaction with nitroso compounds is on-going.

14
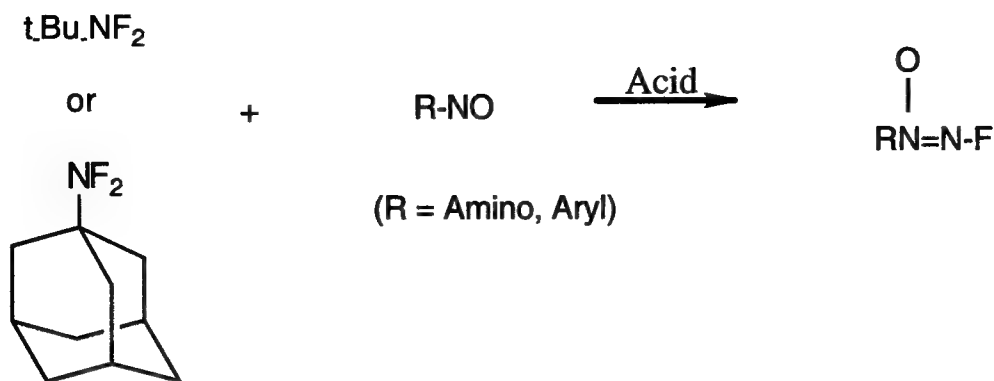
Figure 21. Fluoroazoxy arene and alkane synthesis.

ATTEMPTS AT α-FLUORO NITROSAMINES AND FLUOROAZOXY ALKANES

A fluoroazoxy or fluoronitrosamine species may be useful in creating N-N bonds. The flourination of t-butyl diazenium oxide was attempted as shown in Figure 22. A fast moving volatile product from reaction with F-N(SO2Ph)2 was observed on the TLC plate using EtAc as eluent.
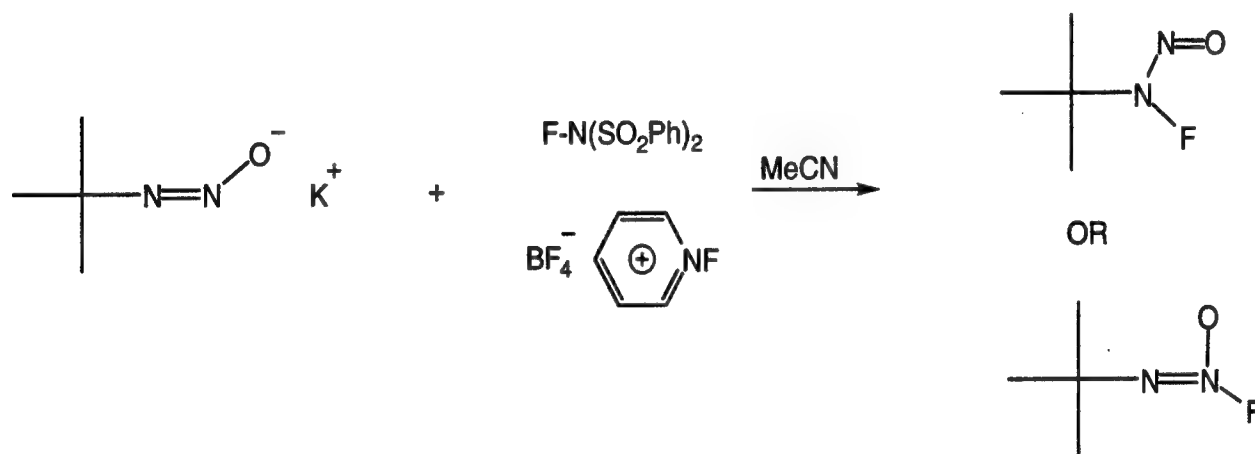
Figure 22. Attempted synthesis of fluoronitrosamine.

Attempts to isolate this product by high temperature (50-60C) distillition have decomposed the product. Other attempts to isolate and characterize this product are ongoing. Attempts to generate t-butyl or 1-adamantyl fluoronitrosoamines via the nitrosation of the monofluoroamines is on-going.

15

CONCLUSIONS

The diazanitrate is not readily acceeded by addition of conventional nitrene equivalents to nitrosamines. Needless to say, the possible repertoire of substrates, reagents, and conditions is vast, and this strategy cannot be dismissed at this stage of the endeavor. The N-nitroazoxy amine, in spite of its close structural relationship to the dinitramide ion, has not so far been synthesized from dinitramide salts. Efforts along these lines will be continued, using O-silyl dinitramide derivatives in reactions with N-silylated amines in an attempt to exploit the strong affinity of silicon for oxygen as the driving force for the replacement of the N-O bond of dinitramide with the N-N bond of the unprecedented N-nitroazoxy amine, $R_2NN(O)NNO_2$.

Analogous reactions have been attempted with the trinitromethane anion, based on its close structural relationship with dinitramide anion. In these reactions, the unprecedented dinitronitronyl amine, $(O_2N)_2CN(O)NR_2$, could not be obtained either. Reactions of O-silylated trinitromethane (Figure 23) behaved similarly.

Figure 23. Dinitronitronyl amine attempted synthesis.

The synthesis of unprecedented oxy-anions if nitrogen, such as nitroazoxy nitramide anion (Figure 24) and di(nitroazoxy) amide (Figure 25), both depend upon the development of

synthesis methodology for the exchange of N—O bonds for N—N bonds in oxidized conjugated systems, such as dinitramide. Once such methods can be developed, the path is clear for the

$$O_2N\text{——}N\text{==}N\text{——}N\text{——}NO_2$$

synthesis of a number of oxy-anions of nitrogen as well as their covalent organic derivatives.
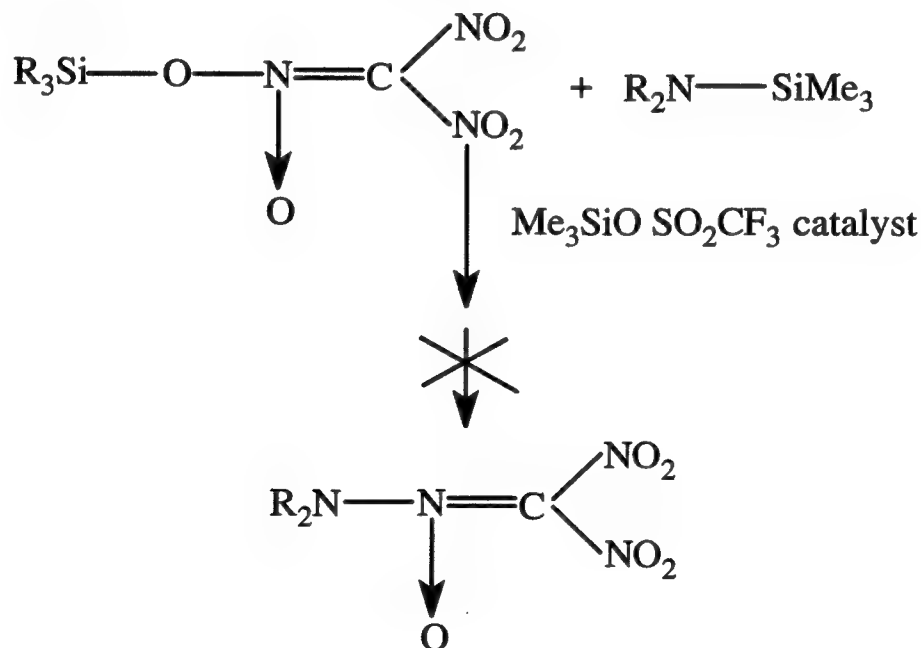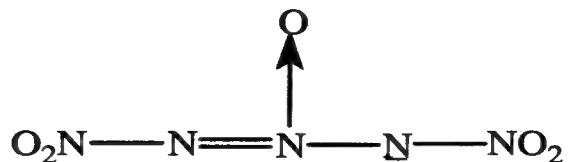
Figure 24. Nitroazoxy nitramide.

$$O_2N\text{——}N\text{==}N\text{——}\overset{\ominus}{N}\text{——}N\text{==}N\text{——}NO_2 \quad (M^+)$$
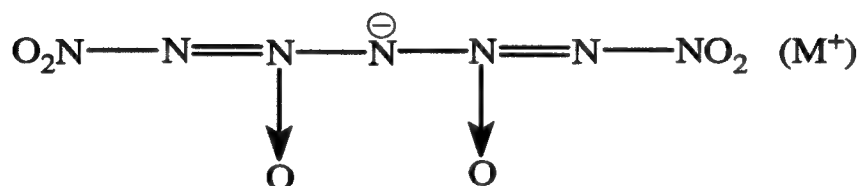
Figure 25. bis(nitroazoxy) amide.

The absence of a metathesis reaction enabling the replacement of N—O bonds of the nitro function with N—N bonds will continue to be an impediment to the development of energetic materials based on $N_xO_y^{z-}$ systems as long as a direct or indirect solution to this problem remains beyond our reach. The Wittig reaction and its nitrogen counterpart enable facile replacement of C—O bonds with C—C and C—N bonds; unfortunately, nitrogen is not so cooperative.

Hydroxynitrourea and its salts show promise as oxidizer and monopropellants, respectively. The advantages of HNU are that it is highly overoxidized and easily prepared with excellent density and crystallinity. Its disadvantages are its marked acidity and its rapid burn rate under elevated pressures. Although preliminary strand and small motor burning studies were not encouraging, it is hoped that formulation technology will surmount this problem. The most hopeful salt of HNU is the ammonium salt; it is insensitive to impact and is oxidatively balanced. Given that its combustion products consist mainly of water, it may be of use as a gun propellant. It has an indefinite shelf-life and shows no evidence of being sensitive to light.

The hydrazinium and hydroxyl ammonium salt of HNU are not as well-behaved; they are somewhat hygroscopic and burn unpredictably; in addition, they display poor density.

Nevertheless, the possibility of a well-behaved eutectic composed of any or all of the above described materials remains to be explored.

The triazanitrate is the least rigorously studied functional group in this program. It will be approached by reacting t-butyllithium with t-butyl azide to give 1,3-bis(t-butyl)-1,2,3-triazapropene, which can be reacted with a varity of electrophillic nitrene precursors. The high valency of the triazanitrate function hold the most promise for simultaneously satisfying the goals of high energy, high density, and high oxygen-content.

The N-oxides of tetrazoles, while in the early stages of investigation, hold tremendous promise because of their close structural relationship with the benzo-1,2,3,4-tetrazines developed by the Soviets. It may very well turn out that these materials have already been made and are being concealed due to their advantageous properties.

The oxidized pentazoles, diazenium diolates, and N-nitroimine ylides remain untouched, both as final products and as reagents for synthesis of more elaborate target products. It may be possible to synthesize these from nitric oxide and amine or hydroxylamine derivatives; this makes them all more attractive.

All in all, more questions have been opened than resolved; this is not unusual in the early stages of any research endeavor. It is hoped that the following phases of this program will rectify this situation.

EXPERIMENTAL

SYNTHESIS OF HYDROXYNITROUREA (1 MOLE-SCALE)

Ammonium nitrourethane (U.S. Patent No. 5,254,324; 1993) (152 g, 1 mole) was dissolved/suspended in 1/2 liter of methanol. To this was added a solution of 1 mole of NaOH in 1 liter of methanol with ice cooling and vigorous stirring to prevent side reactions arising from unintentional local high concentrations of base. When the addition was complete, all solvent was evaporated in vacuo to remove excess NH_3. This was then dissolved in 500 mL MeOH. Next, a solution of 1.1 moles of NH_2OH (as a 50% aqueous solution) was dissolved in 500 mL CH_3OH. The sodium nitrourethane solution and the sodium hydroxide/hydroxylamine solution were combined quickly and stirred vigorously. There was an immediate precipitate of the disodium salt of HNU. Next, 1.05 moles of H_2SO_4 was dissolved in 1/2 liter of CH_3OH and this solution was combined with the suspension of the disodium salt of HNU in CH_3OH. The resulting suspension was stirred for 6 hours at room temperature and was filtered. The filtrate was passed through a 4" x 1" plug of SiO_2 eluting with CH_3OH. The effluent was concentrated in vacuo to approximately 500 mL, at which point a heavy precipitate of needles was noted. It was placed in a freezer at –10°C for 3 hours and filtered. The solid isolated was dried in vacuo (yield = 60 g = 50%). The mother liquor was concentrated to 250 mL and diluted to 500 mL with i-pr-OH. The resulting precipitate was filtered, yielding approximately 30 g of solid having acceptable properties (negligible burn residue, good crystal morphology). The total nonoptimized yield was 90 g ~ 75%.

SYNTHESIS OF AMMONIUM HYDROXYNITROUREA

Hydroxynitrourea (12 g, 100 mmol) was dissolved in 200 mL of methanol and treated with an excess of NH_3 gas (6 g, 300 mmol). An amorphous precipitate was observed immediately; this was stirred for 15 min and filtered to give 13 g (95%) Differential Scanning Calorimetry decomposition occurred sharply at 155°C. This material was not hygroscopic and could not be detonated by a sharp hammer blow. Its x-ray crystal structure showed a density of approximately 1.8 g/cc. A variety of other salts of HNU were prepared and DSC data were obtained on these, too. None showed the promise of HNU or ammonium HNU.

Alternatively, 24 g (200 mmol) of HNU was dissolved in 300 mL of methanol (with warming) and treated with 13 g of commercial 30% aqueous ammonia. The resulting neutral

solution was stirred for 10 seconds and allowed to stand at room temperature for 1 hour, during which 28 g (94%) of needles precipitated. This product was filtered and dried.

NITROBIURET: A SIMPLE TEST PLATFORM FOR THE DEVELOPMENT OF N – O/N = N METATHESIS METHODOLOGY
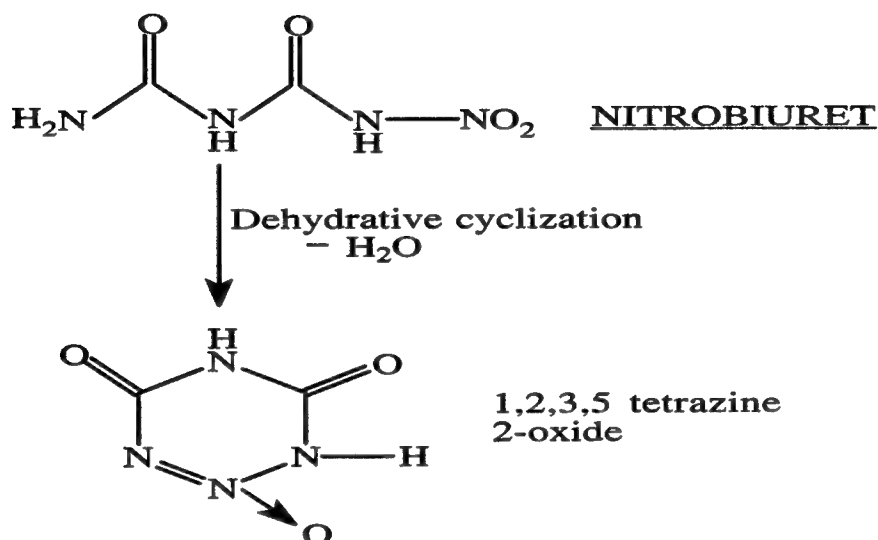
Figure 26. Dehydrative cyclization of nitrobiuret.

The diazanitrate function can appear in a myriad of contexts and can be approached by a plethora of methods. It was hoped that the dehydrative cyclization of nitrobiuret would result in a 6-pi-electron aromatic system whose enthalpic and entropic attributes would operate synergistically to bring about its formation under a carefully optimized set of conditions. In our preliminary efforts, nitrobiuret was treated with titanium isopropoxide and heated to 100°C; no obvious reaction occurred, as determined by TLC. Next, it was exhaustively silylated and treated with a catalytic quantity of trimethylsilyl trifluoromethane sulfonate at 100°C in order to effect an acid-catalyzed anhydrous cyclization; again, no obvious reaction occurred, as assayed by TLC. Next, triethyl ammonium nitrobiuret (a stable salt) was treated with diethyl chlorophosphate, in an effort to phosphorylate one of the oxygenations of the nitramine and drive the cyclization; again, no obvious reaction occurred, as assayed by TLC. This preliminary study was abandoned and higher priority endeavors were pursued.

20

FUTURE DIRECTIONS, POSSIBILITIES, AND PRIORITIES

Many promising but nevertheless incomplete results arose from the work described in this report. The erratic behavior of the nitrosamine is by no means justification for abandonment of this methodological path to the diazanitrate functions. It will almost certainly by productive to explore variations in the conditions of reactions leading to the diazanitrate, especially those involving intramolecular templates.

The diazenium diolate was given at most a cursory examination; close relatives of the diazenium diolate such as the α-fluoronitrosamine, the α-methoxynitrosamine and the α-chloronitrosamine need to be explored as electrophillic participants in reactions leading to the diazanitrate. The use of alkylated products of trimethylamine nitroimine ylides (Figure 27) as a $(+)N = N(+) = 0$ bifunctional electrophile is intriguing; preliminary experiments in this area gave only tarring and decomposition.
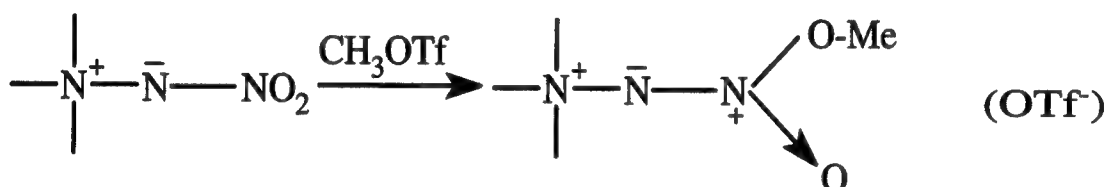
Figure 27. Trimethylamine nitroimine ylide.

The pursuit of tetrazole bis-N-oxide as well as pentazoles by simple addition of nitric oxide to amidine, hydrazine, or even hydroxylamine precursors, followed by cyclization, is another intriguing possibility. The Russian success with 1,2,3,4-tetrazine-1,3 N-oxides confers validity on the pentazole 1,3 N-oxides as stable targets based on simple electronic arguments (see Figure 28).
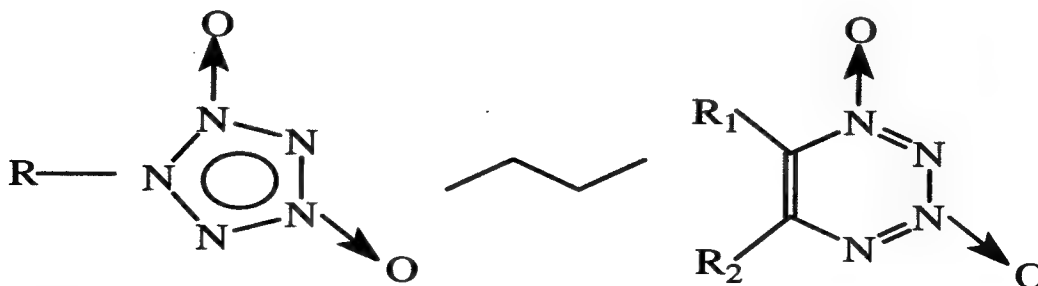
Figure 28. Quantum-mechanical similarity between pentazole 1,3-bis-N-oxides and 1,2,3,4-tetrazene-1,3-bis N-oxides.

21

Also, addition of azide ion to α-fluoro-nitrosamines (see Figure 29) is a mechanistically promising path to pentazole-2-oxides.

Figure 29. Pentazole synthesis via azide reaction to α-fluoronitrosamines.

Finally, the adduct of tert-butyllithium with tert-butyl azide serves as an elegant segway to triazanitrate by addition of nitrene equivalents to the central nitrogen of that anionic diazanitrite analogue (see Figure 30). A comprehensive study will be made of the reactivity of this system with nitrene precursors compatible with its strong basicity.

Figure 30. Possible access to triazanitrate system.
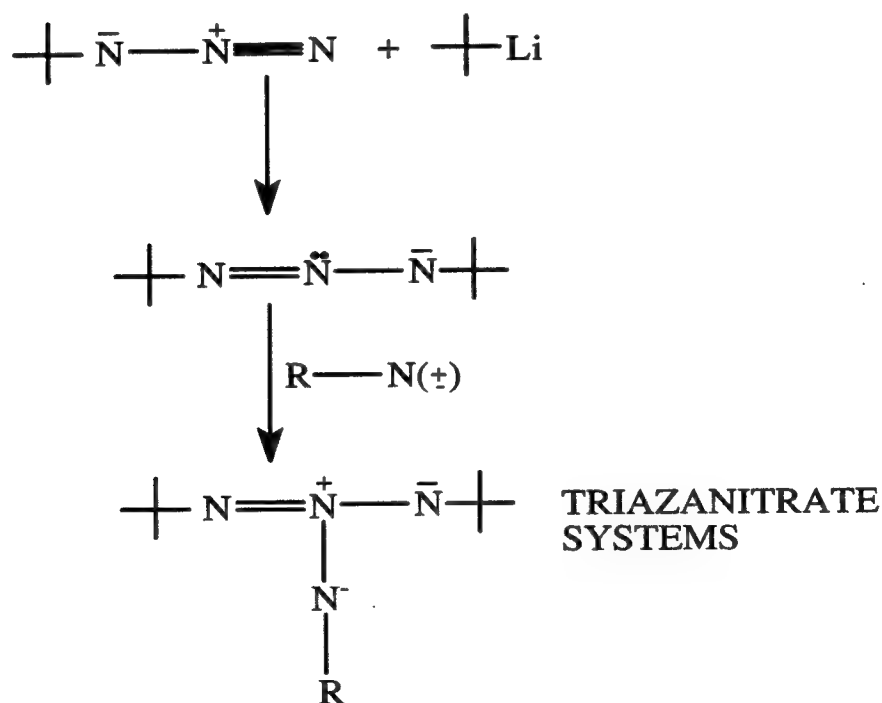
22

REACTIONS ATTEMPTED WITH 4-NITROSO-N,N,-DIMETHYLANILINE

The brilliant green commercially available 4-nitroso-N,N-dimethylaniline (Figure 31) was used for a number of experiments modeling the electron-rich nitroso group. It was found that silylation of this material with trimethylsilyl triflate gave a pale orange salt, presumed to be the O-silylated derivative shown in Figure 32.
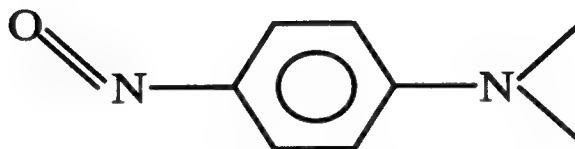
Figure 31. 4-Nitroso-N.N-dimethylaniline.
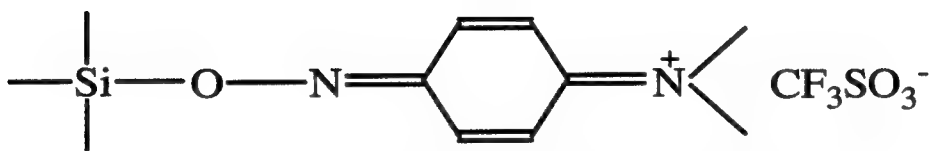
Figure 32. Trimethylsilyl triflate salt of 4-nitroso-N,N-dimethylaniline.

This demonstrated the nitrosamine-like electronics of this material; as a consequence, it was used in place of dimethylnitrosamine to model the properties of the highly toxic nitrosamines.

The addition of silver dinitramide to 4 NND (acronym for 4-nitroso-N,N-dimethyl(aniline) was intended to generate the nitroazoxy derivative; in fact, a plethora of products was created by this reaction, most were unstable and were not readily characterizable. The work involving reactions of trinitromethane salts and dinitramine salts with aromatic aldehydes to give dinitronitrone and nitroazoxy derivatives, respectively was abandoned pending further methodological advances.

23

APPENDIX A

X-RAY STRUCTURE HNU

Table 1. Crystal data and structure refinement for bott72m.

Identification code	bott72m
Empirical formula	C H3 N3 O4
Formula weight	121.06
Temperature	293(2) K
Wavelength	0.71073 Å
Crystal system	Orthorhombic
Space group	P2(1)2(1)2(1)
Unit cell dimensions	a = 4.7116(4) Å $\alpha= 90°$.
	b = 6.9585(6) Å $\beta= 90°$.
	c = 12.8495(11) Å $\gamma = 90°$.
Volume	421.28(6) $Å^3$
Z	4
Density (calculated)	1.909 Mg/m^3
Absorption coefficient	0.192 mm^{-1}
F(000)	248
Crystal size	0.40 x 0.18 x 0.23 mm^3
Theta range for data collection	3.17 to 25.33°.
Index ranges	-5<=h<=4, -8<=k<=8, -14<=l<=15
Reflections collected	1852
Independent reflections	768 [R(int) = 0.0218]
'Observed' independent reflections	744 [I(obs) > 2σ(I)]
Completeness to theta = 25.33°	99.8%
Absorption correction	Integration
Max. and min. transmission	0.9737 and 0.9522
Refinement method	Full-matrix least-squares on F^2
Data / restraints / parameters	768 / 0 / 78
Goodness-of-fit on F^2	1.071
Final R indices [I>2sigma(I)]	R1 = 0.0271, wR2 = 0.0757
R indices (all data)	R1 = 0.0280, wR2 = 0.0763
Absolute structure parameter	1(2)
Extinction coefficient	0.096(13)
Largest diff. peak and hole	0.195 and -0.248 $e.Å^{-3}$

Table 2. Atomic coordinates (x 10^4) and equivalent isotropic displacement
parameters (Å^2x 10^3) for bott72m. U(eq) is defined as
one third of the trace of the orthogonalized U^{ij} tensor.

	x	y	z	U(eq)
N(1)	-2080(4)	1263(2)	8956(1)	31(1)
O(1)	-172(3)	2769(2)	9074(1)	38(1)
C(2)	-1341(4)	-134(2)	8314(1)	24(1)
O(2)	679(3)	-43(2)	7702(1)	29(1)
N(3)	-2943(3)	-1816(2)	8275(1)	29(1)
N(3A)	-5063(3)	-2378(2)	8930(1)	28(1)
O(3A)	-5915(3)	-4015(2)	8798(1)	42(1)
O(3B)	-5945(3)	-1247(2)	9577(1)	34(1)

Table 2a. Hydrogen coordinates (x 10^4) and isotropic displacement
parameters (Å^2 x 10^3) for bott72m.

	x	y	z	U(eq)
H(1A)	-3668	1241	9286	37
H(3A)	-2546	-2595	7777	34
H(1)	-740(70)	3550(40)	8590(20)	73(9)

Table 3. Bond lengths [Å] and angles [°] for bott72m.

N(1)-C(2)	1.322(2)	N(3)-N(3A)	1.364(2)
N(1)-O(1)	1.3888(19)	N(3A)-O(3B)	1.2176(18)
C(2)-O(2)	1.236(2)	N(3A)-O(3A)	1.2195(17)
C(2)-N(3)	1.394(2)		

C(2)-N(1)-O(1)	116.89(15)
O(2)-C(2)-N(1)	124.23(16)
O(2)-C(2)-N(3)	115.94(14)
N(1)-C(2)-N(3)	119.79(16)
N(3A)-N(3)-C(2)	128.03(14)
O(3B)-N(3A)-O(3A)	125.91(15)
O(3B)-N(3A)-N(3)	119.06(14)
O(3A)-N(3A)-N(3)	115.03(14)

Table 4. Anisotropic displacement parameters ($\text{Å}^2 \times 10^3$) for bott72m.
The anisotropic displacement factor exponent takes the
form: $-2\pi^2[\, h^2\, a^{*2}U^{11} + ... + 2\, h\, k\, a^*\, b^*\, U^{12}\,]$

	U^{11}	U^{22}	U^{33}	U^{23}	U^{13}	U^{12}
N(1)	39(1)	24(1)	30(1)	-5(1)	6(1)	-5(1)
O(1)	58(1)	25(1)	30(1)	-1(1)	-3(1)	-13(1)
C(2)	28(1)	21(1)	22(1)	3(1)	-1(1)	1(1)
O(2)	31(1)	26(1)	29(1)	1(1)	5(1)	-1(1)
N(3)	32(1)	25(1)	29(1)	-5(1)	9(1)	-3(1)
N(3A)	25(1)	30(1)	27(1)	1(1)	-2(1)	-2(1)
O(3A)	46(1)	35(1)	45(1)	-6(1)	6(1)	-17(1)
O(3B)	34(1)	37(1)	30(1)	-6(1)	7(1)	1(1)
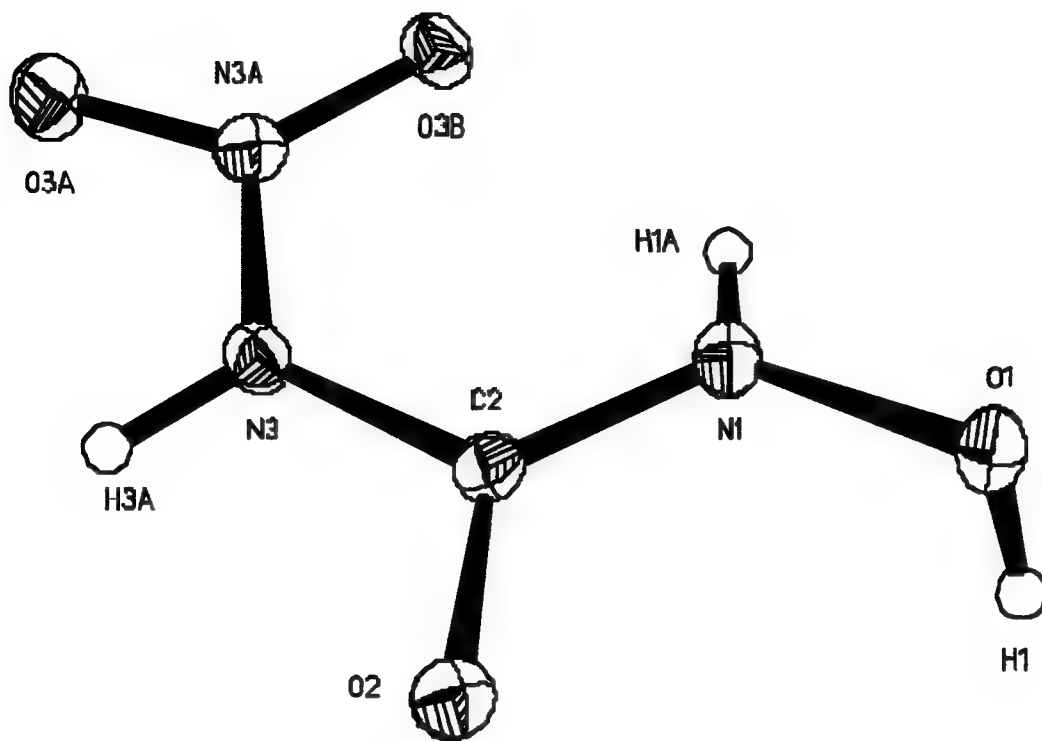
An ORTEP drawing from an X-ray analysis at the Naval Research Laboratory (Gilardi, 12/06/00).
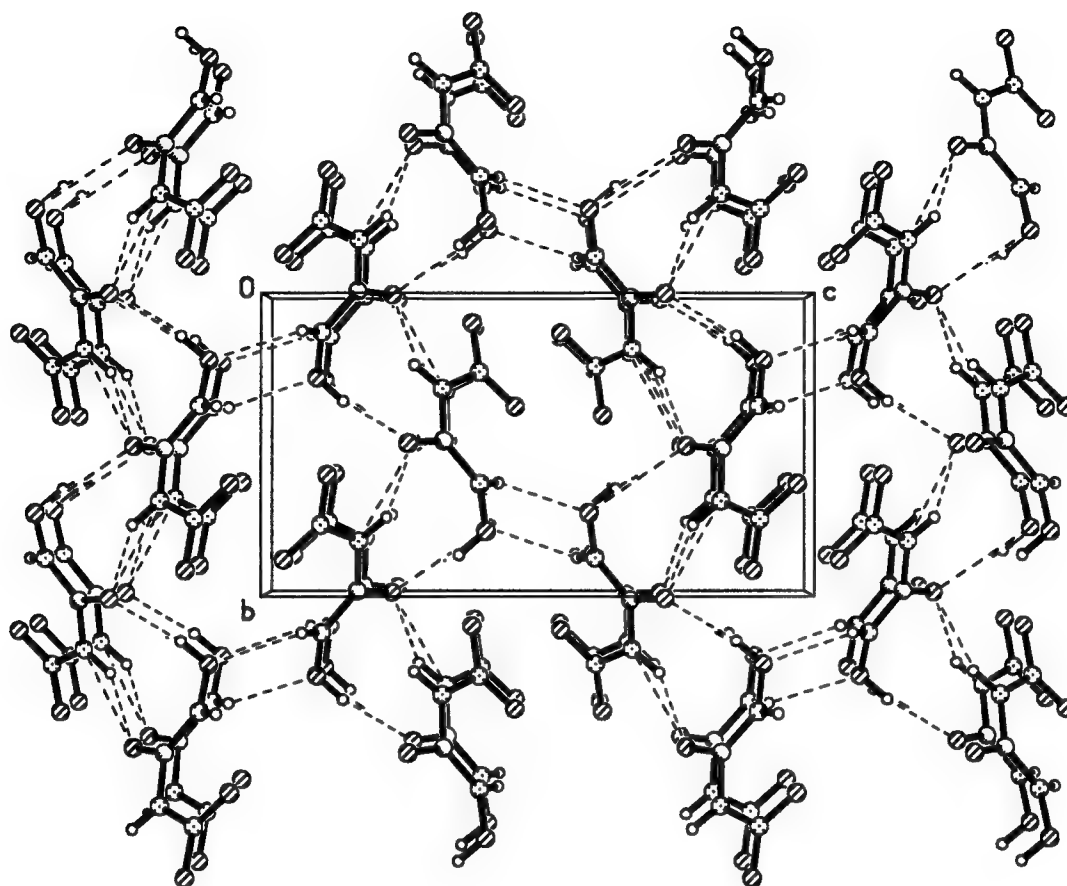
View of hydroxynitrourea in the crystal, down the short a axis of the cell. The strongest (i.e, shortest, straightest) H-bonds involve the OH hydrogen, the carbonyl oxygen, and the NH adjacent to the nitro group. This is what would be expected from predictions of the most polar regions of the molecule. This set of H-bonds connects the molecules into ribbons. A stack of two such ribbons can be seen above in the region to the left of the unit cell, and other parallel ribbons fill in the rest of the diagram. As you can see, there are also weaker H-bonds connecting the ribbons to one another. In the next figure, a single ribbon is taken out and shown from two directions. Although the above diagram appears flat, it is not, as will be seen later in a view down the b axis.
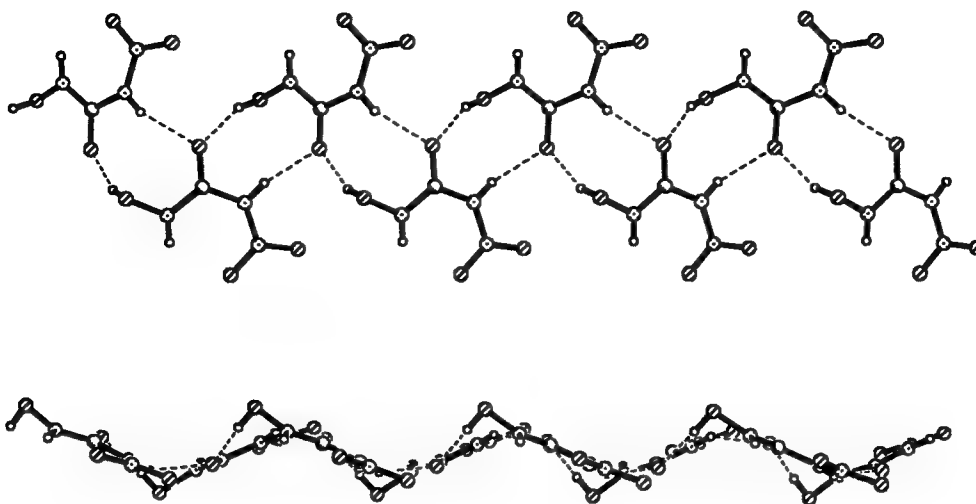
Two views of the tightly bonded "ribbon motif" of hydroxynitrourea. The symmetry generator that relates the molecules and 'generates the ribbon' is a two-fold screw axis along the b axis. The ribbon is crinkled, probably to optimize H-bond energies.
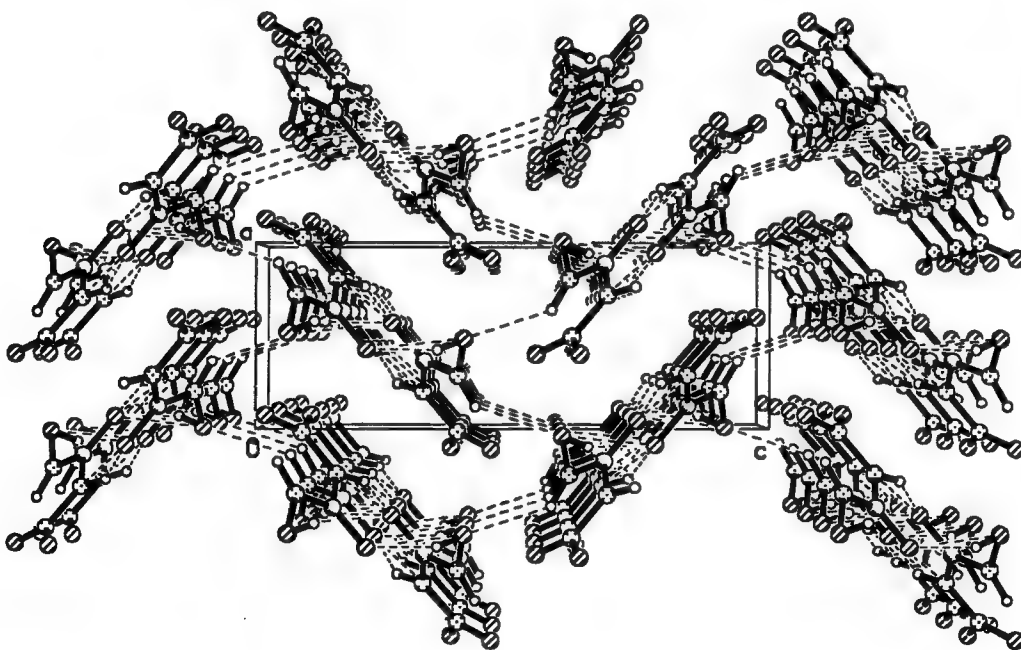
This is a view down the b axis, which is down the axes of the tightly-bonded ribbons, so they are seen end-on . A ribbon is not surrounded by parallel neighboring ribbons (except in the short a direction), so there are no extended sheets and no obvious cleavage planes in this crystal, as are seen in TATB and several other insensitive aromatic compounds. [FOX-7 shows somewhat wavy H-bonded sheets in the crystal, but they are still recognizable as extended sheets.]

APPENDIX B

HNU EVALUATION

Subject: HNU and Ammonium HNU Safety Properties
    Date: Mon, 29 Jul 2002 08:40:42 -0700
    From: "Ciaramitaro, Dave" <CiaramitarDA@navair.navy.mil>
      To: "'Jeffrey C Bottaro'" <jeffrey.bottaro@sri.com>

Jeff,

We finally finished evaluating HNU and the ammonium salt in some propellant formulations and found them both to be thermally incompatible. Our Vacuum Thermal Stability test, even when run at 80°C, appeared to induce a gassing reaction in binders such as GAP, PGN and BAMO/NMMO. In the formula using PGN, the reaction could be much more violent. A formulation with this binder had both samples explode within a few minutes of each other. We did DSCs of the HNU with each of the other ingredients and found nothing particularly alarming.

Our analyst then got hold of software which would allow a DSC sample to be held at a given temperature, instead of being ramped up at a given rate, as the DSC is normally done. I gave her samples of HNU in combination with two other ingredients which we have been using in our formulations. We stayed with PGN as the binder because that gave the most violent reaction in the VTS. These mixtures were held at 80°C for 24 hours with the following results:

MIXTURE	TIME TO EXOTHERM(s)
HNU, PGN, BTTN	16 hours; 17 hours
HNU, BTTN, AN	7 hours; 9 hours; endotherm at 5 hours
HNU, PGN, AN at 4-1/4 hours	4 hours; 5-1/2 hours; 7-1/4 hours; endotherm
HNU, PGN, ADN	Jagged base line; no definite exotherm
HNU, PGN, CL-20	15 hours; 16 hours
HNU, PGN, N-100	No exotherm; endotherm at 3-1/4 hours
HNU, BTTN, ADN	Jagged base line; slow exotherm at 14 hours
HNU, BTTN, CL-20	Slight exotherms at 2 and 6 hours
HNU, BTTN, N-100	Slow, slight at 7 and 8-1/2 hours
HNU, AN, ADN	2 hours; 5 hours
HNU, AN, CL-20	5 hours; 7 hours; endotherm at 3-1/2 hours
HNU, AN, N-100	endotherms at 2-1/2 and 9 hours
HNU, ADN, CL-20	14 hours Slow, mild; mild at 16 hours
HNU, ADN, N-100	Endotherms at 2 and 9 hours
HNU, CL-20, N-100	Endotherm at 8 hours

Unless otherwise indicated, the typical first exotherm is a somewhat broad, but large peak, taking about 3 hours to fully develop, followed by a sharp spike of perhaps a quarter-hour's duration.

From the looks of things, mixing HNU with AN and any other energetic material gave the potential for a large energy release. The two in

combination with an inert material such as N-100, gave much milder reactions. Mixing HNU and PGN with BTTN or CL-20 would also result in good-sized exotherms, but these, although considerable, were somewhat smaller and occurred later than the ones with AN. Why such an innocuous material as AN in combination with HNU should be so reactive while such species as ADN and CL-20 were noticeably less so, is kind of an odd circumstance.

We are trying to coat the HNU material in an effort to use it. But at present, although it does not seem thermally unstable itself, it can be quite reactive, and thus thermally incompatible, in combination with other formulation ingredients.

APPENDIX C

DSC COMPARISON OF HYDROXYNITROUREA SALTS

DSC Comparison of Hydroxynitrourea salts

Carbohydrazidium HNU
Formamidinium HNU
Guanidinium HNU
HNU
Ammonium HNU
Amino Guanidinium HNU
Hydroxylammonium HNU

156.47°C
153.55°C
149.07°C
131.59°C
128.75°C
124.96°C
107.96°C

HNU
NH4+ HNU
FORMAMIDINIUM HNU
Guanidinium HNU
AMINO GUANIDINIUM HNU
H2N-N(H2+
H3NOH+ HNU

Heat Flow (mW)

Temperature (°C)

Exo Up

Universal V2.6D TA Instruments

C-2
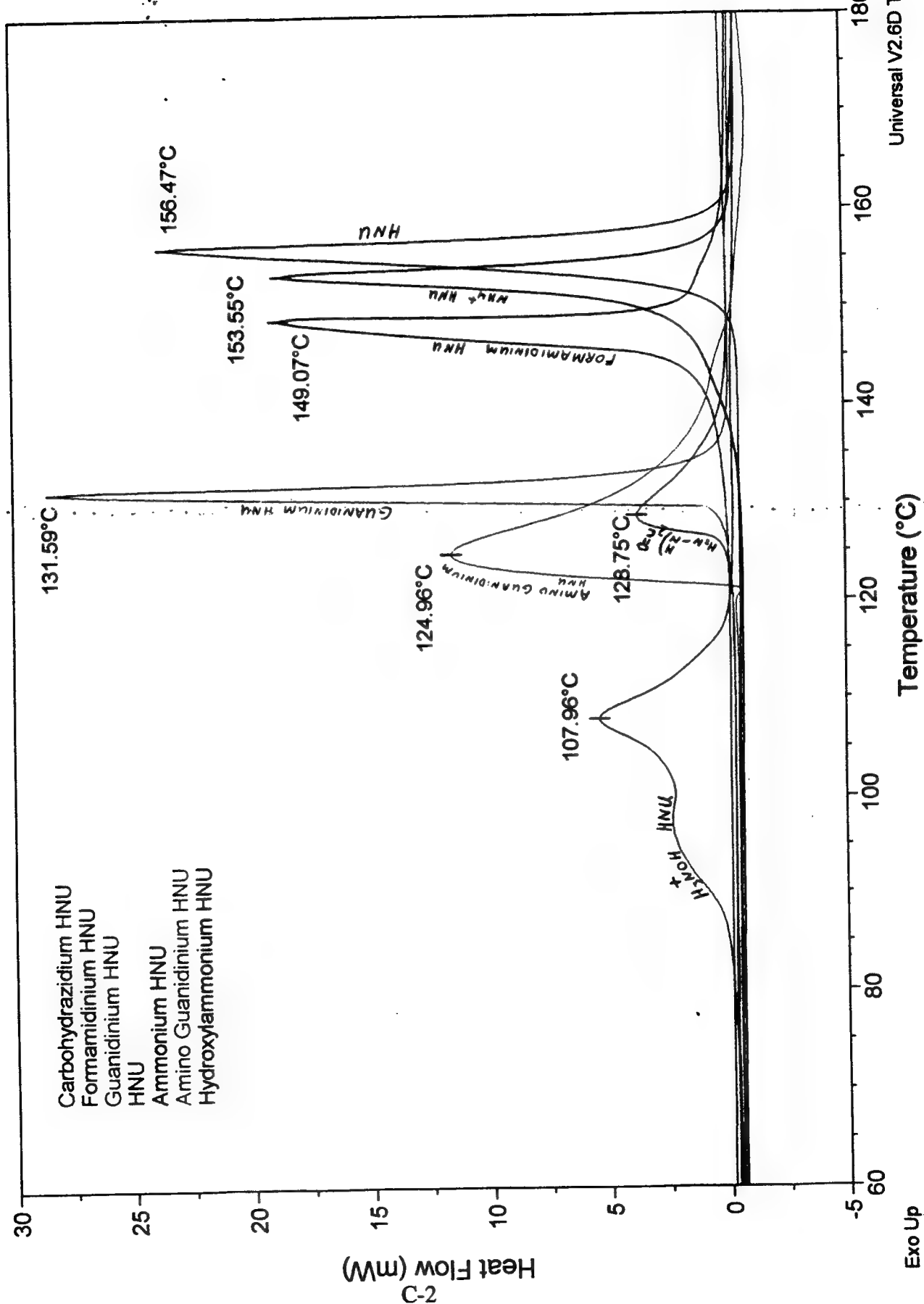
APPENDIX D

AMMONIUM HNU

Fig. 1. All atoms show up clearly.

Fig. 2. Contents of one unit cell. Some H-bonds are shown here, but the strongest H-bonds occur between molecules in adjacent unit cells.
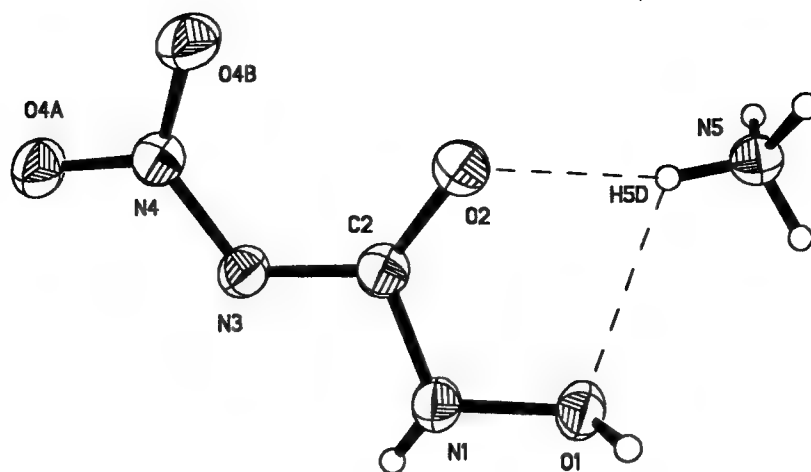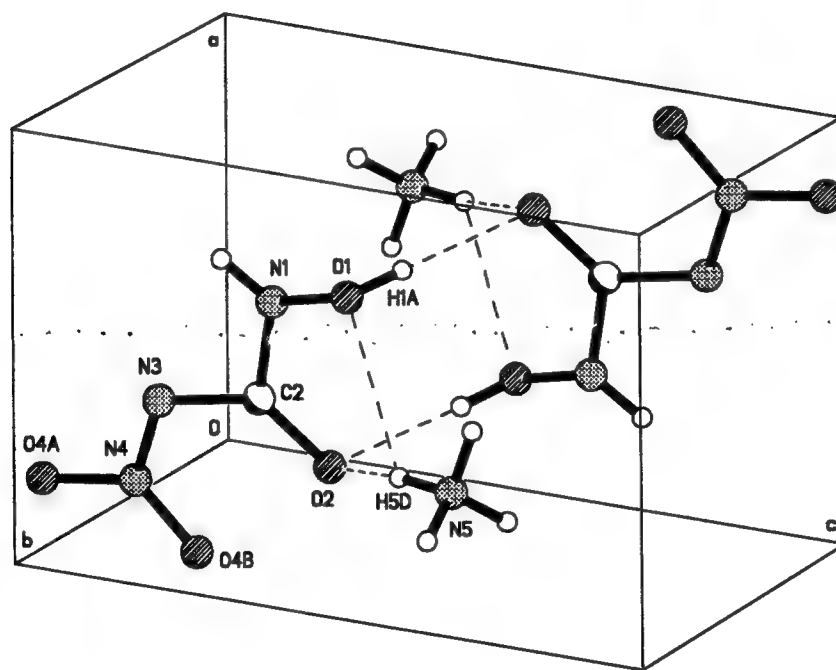
Table 1. Crystal data and structure refinement for srip09m.

Identification code	srip09m	
Empirical formula	C H6 N4 O4	
Formula weight	138.10	
Temperature	293(2) K	
Wavelength	1.54178 Å	
Crystal system	Triclinic	
Space group	P-1	
Unit cell dimensions	a = 5.3765(4) Å	α= 109.873(4)°.
	b = 6.7723(5) Å	β= 100.217(4)°.
	c = 7.9155(5) Å	γ = 102.520(4)°.
Volume	254.52(3) Å^3	
Z	2	
Density (calculated)	1.802 Mg/m^3	
Absorption coefficient	1.573 mm^{-1}	
F(000)	144	
Crystal size	0.24 x 0.14 x 0.04 mm^3	
Theta range for data collection	6.18 to 66.91°.	
Index ranges	-6<=h<=6, -8<=k<=7, -9<=l<=9	
Reflections collected	2063	
Reflections 'observed'	827 [I>2sigma(I)]	
Independent reflections	852 [R(int) = 0.0207]	
Completeness to theta = 66.91°	93.7 %	
Absorption correction	Multiscan	
Max. and min. transmission	0.9398 and 0.7279	
Refinement method	Full-matrix least-squares on F^2	
Data / restraints / parameters	852 / 0 / 87	
Goodness-of-fit on F^2	1.135	
Final R indices [I>2sigma(I)]	R1 = 0.0426, wR2 = 0.1053	
R indices (all data)	R1 = 0.0429, wR2 = 0.1058	
Extinction coefficient	0.225(18)	
Largest diff. peak and hole	0.295 and -0.424 e.Å^{-3}	

Table 2. Atomic coordinates (x 10^4) and equivalent isotropic displacement parameters ($Å^2$x 10^3)
for srip09m. U(eq) is defined as one third of the trace of the orthogonalized U^{ij} tensor.

	x	y	z	U(eq)
O(1)	6320(2)	6944(2)	4291(1)	40(1)
N(1)	5309(3)	5246(2)	2513(2)	37(1)
C(2)	2653(3)	4270(2)	1950(2)	30(1)
O(2)	1347(2)	4286(2)	3092(1)	40(1)
N(3)	1868(2)	3329(2)	19(2)	33(1)
N(4)	-565(2)	1976(2)	-834(2)	32(1)
O(4A)	-1172(2)	1222(2)	-2583(1)	45(1)
O(4B)	-2209(2)	1410(2)	-50(1)	52(1)
N(5)	2910(2)	8889(2)	6593(1)	39(1)

Table 3.   Bond lengths [Å] and angles [°] for srip09m.

O(1)-N(1)	1.3984(16)	N(4)-O(4B)	1.2337(15)
O(1)-H(1A)	0.82(2)	N(4)-O(4A)	1.2532(15)
N(1)-C(2)	1.356(2)	N(5)-H(5A)	0.9000
N(1)-H(1)	0.82(2)	N(5)-H(5B)	0.9001
C(2)-O(2)	1.2379(17)	N(5)-H(5C)	0.9000
C(2)-N(3)	1.3833(17)	N(5)-H(5D)	0.9000
N(3)-N(4)	1.3240(17)		
N(1)-O(1)-H(1A)	107.3(14)	O(4B)-N(4)-N(3)	125.45(11)
C(2)-N(1)-O(1)	116.28(11)	O(4A)-N(4)-N(3)	115.38(12)
C(2)-N(1)-H(1)	122.0(14)	H(5A)-N(5)-H(5B)	109.5
O(1)-N(1)-H(1)	111.2(14)	H(5A)-N(5)-H(5C)	109.5
O(2)-C(2)-N(1)	121.38(13)	H(5B)-N(5)-H(5C)	109.5
O(2)-C(2)-N(3)	130.39(14)	H(5A)-N(5)-H(5D)	109.5
N(1)-C(2)-N(3)	108.22(12)	H(5B)-N(5)-H(5D)	109.5
N(4)-N(3)-C(2)	118.57(11)	H(5C)-N(5)-H(5D)	109.4
O(4B)-N(4)-O(4A)	119.16(11)		

Table 4. Anisotropic displacement parameters $(\text{Å}^2 \times 10^3)$ for srip09m. The anisotropic displacement factor exponent takes the form: $-2\pi^2[h^2 a^{*2}U^{11} + \dots + 2hk\,a^*\,b^*\,U^{12}]$

	U^{11}	U^{22}	U^{33}	U^{23}	U^{13}	U^{12}
O(1)	40(1)	41(1)	27(1)	7(1)	4(1)	2(1)
N(1)	32(1)	45(1)	24(1)	7(1)	8(1)	2(1)
C(2)	31(1)	31(1)	29(1)	12(1)	9(1)	8(1)
O(2)	35(1)	50(1)	30(1)	13(1)	12(1)	6(1)
N(3)	28(1)	37(1)	27(1)	10(1)	6(1)	2(1)
N(4)	31(1)	32(1)	29(1)	10(1)	7(1)	8(1)
O(4A)	42(1)	53(1)	26(1)	8(1)	3(1)	5(1)
O(4B)	36(1)	65(1)	39(1)	15(1)	12(1)	-7(1)
N(5)	34(1)	39(1)	38(1)	12(1)	11(1)	6(1)

Table 5. Hydrogen coordinates (x 10^4) and isotropic displacement parameters ($\text{Å}^2 \times 10^3$) for srip09m.

	x	y	z	U(eq)
H(1A)	6990(40)	6440(30)	5000(30)	48
H(1)	6140(40)	5490(30)	1790(30)	44
H(5A)	2203	8169	7246	58
H(5B)	2086	9897	6534	58
H(5C)	4647	9566	7162	58
H(5D)	2703	7924	5430	58

Table 6. Torsion angles [°] for srip09m.

O(1)-N(1)-C(2)-O(2)	-24.57(18)
O(1)-N(1)-C(2)-N(3)	156.43(11)
O(2)-C(2)-N(3)-N(4)	-10.0(2)
N(1)-C(2)-N(3)-N(4)	168.92(11)
C(2)-N(3)-N(4)-O(4B)	-2.40(19)
C(2)-N(3)-N(4)-O(4A)	178.36(11)

Table 7. Hydrogen bonds for srip09m [Å and °].

| D-H...A	d(D-H)	d(H...A)	d(D...A)	<(DHA)
O(1)-H(1A)...O(2)#1	0.82(2)	1.88(2)	2.6953(14)	171.2(19)
N(1)-H(1)...N(3)#2	0.82(2)	2.19(2)	3.0018(18)	169.5(18)
N(5)-H(5A)...O(2)#3	0.90	2.15	2.8906(13)	139.2
N(5)-H(5A)...O(4B)#3	0.90	2.14	2.8951(16)	141.1
N(5)-H(5B)...O(4A)#4	0.90	2.25	3.0079(16)	142.0
N(5)-H(5C)...O(4A)#5	0.90	2.22	3.0709(15)	156.7
N(5)-H(5C)...O(4B)#5	0.90	2.27	3.060	145.6
N(5)-H(5D)...O(1)	0.90	2.41	3.0029(14)	123.6
N(5)-H(5D)...O(2)	0.90	2.38	3.2044(14)	152.1

Symmetry transformations used to generate equivalent atoms:

#1 -x+1,-y+1,-z+1   #2 -x+1,-y+1,-z   #3 -x,-y+1,-z+1

#4 x,y+1,z+1   #5 x+1,y+1;z+1

APPENDIX E

X-RAY STRUCTURE OF T-BUTYL PIVALOYL TRIAZENE
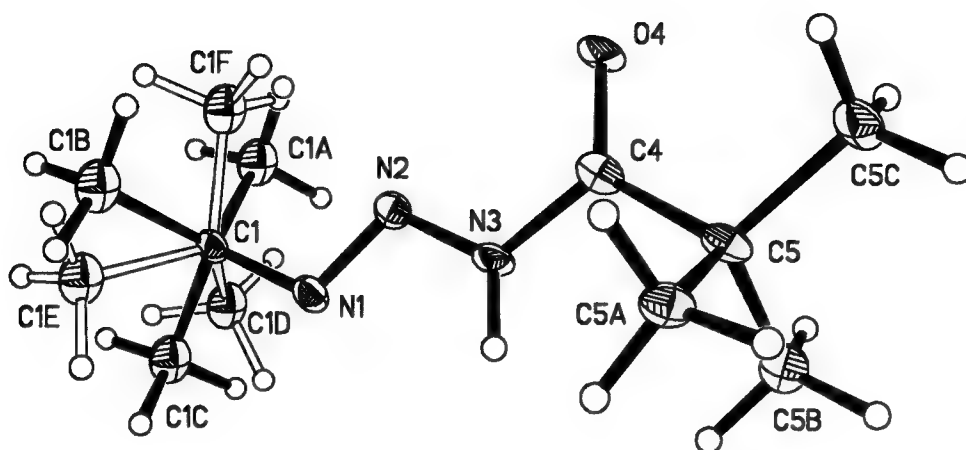
BOTT71: The crystals looked good, but did not diffract too well. I collected at very low Temperature (-170C). Usually that improves the data, but sometimes it cracks the crystals, and maybe that happened here. However, I do get the expected structure, with a wobbling t-butyl group at one end. The H-atom on the central Nitrogen was visible.

Table 1. Crystal data and structure refinement for bott71a.

Identification code	bott71a
Empirical formula	C9 H19 N3 O
Formula weight	185.27
Temperature	99(2) K
Wavelength	0.71073 Å
Crystal system	Monoclinic
Space group	P2(1)/n
Unit cell dimensions	a = 5.819(2) Å $\alpha = 90°$.
	b = 20.219(9) Å $\beta = 103.782(6)°$
	c = 9.788(4) Å $\gamma = 90°$
Volume	1118.5(8) Å^3
Z	4
Density (calculated)	1.100 Mg/m^3
Absorption coefficient	0.074 mm^{-1}
F(000)	408
Crystal size	0.06 x 0.06 x 0.36 mm^3
Theta range for data collection	2.37 to 23.27°.
Index ranges	-6<=h<=2, -12<=k<=22, -9<=l<=10
Reflections collected	2943
Independent reflections	1346 [R(int) = 0.0854]
Completeness to theta = 23.27°	83.6%
Absorption correction	None
Refinement method	Full-matrix least-squares on F^2
Data / restraints / parameters	1346 / 30 / 119
Goodness-of-fit on F^2	0.940
Final R indices [I>2sigma(I)]	R1 = 0.0794, wR2 = 0.2023
R indices (all data)	R1 = 0.1513, wR2 = 0.2297
Largest diff. peak and hole	0.468 and -0.365 e.Å^{-3}

Table 2. Atomic coordinates (x 10^4) and equivalent isotropic displacement
parameters (Å^2x 10^3) for bott71a. U(eq) is defined as
one third of the trace of the orthogonalized U^{ij} tensor.

	x	y	z	U(eq)
N(1)	-2162(7)	1386(3)	7269(5)	31(1)
N(2)	-540(7)	1624(3)	8207(5)	30(1)
N(3)	341(7)	2199(3)	7786(5)	31(1)
C(4)	2181(8)	2515(4)	8658(6)	30(2)
O(4)	3046(6)	2309(2)	9843(4)	35(1)
C(5)	3077(8)	3132(3)	8025(6)	29(2)
C(5A)	3933(9)	2932(3)	6716(6)	32(2)
C(5B)	1074(9)	3641(3)	7643(6)	38(2)
C(5C)	5148(10)	3434(3)	9113(6)	41(2)
C(1)	-3099(7)	756(3)	7646(5)	29(2)
C(1A)	-3363(15)	709(5)	9159(7)	47(2)
C(1B)	-1599(14)	181(4)	7334(10)	47(2)
C(1C)	-5553(11)	723(5)	6640(8)	47(2)
C(1D)	-5675(11)	841(7)	7702(12)	47(2)
C(1E)	-2886(19)	268(6)	6496(10)	47(2)
C(1F)	-1629(17)	517(7)	9067(8)	47(2)

Table 3. Bond lengths [Å] and angles [°] for bott71a.

N(1)-N(2)	1.246(6)	C(5)-C(5A)	1.535(8)
N(1)-C(1)	1.468(7)	C(1)-C(1D)	1.522(5)
N(2)-N(3)	1.373(6)	C(1)-C(1E)	1.524(5)
N(3)-C(4)	1.359(7)	C(1)-C(1F)	1.527(5)
C(4)-O(4)	1.222(6)	C(1)-C(1B)	1.527(5)
C(4)-C(5)	1.538(9)	C(1)-C(1A)	1.527(5)
C(5)-C(5C)	1.533(7)	C(1)-C(1C)	1.531(5)
C(5)-C(5B)	1.533(8)		
N(2)-N(1)-C(1)	114.3(4)	C(1E)-C(1)-C(1F)	110.0(3)
N(1)-N(2)-N(3)	112.2(5)	N(1)-C(1)-C(1B)	110.2(5)
C(4)-N(3)-N(2)	120.2(5)	C(1D)-C(1)-C(1B)	135.1(8)
O(4)-C(4)-N(3)	121.4(6)	C(1E)-C(1)-C(1B)	37.7(5)
O(4)-C(4)-C(5)	123.8(5)	C(1F)-C(1)-C(1B)	73.7(5)
N(3)-C(4)-C(5)	114.8(5)	N(1)-C(1)-C(1A)	115.3(5)
C(5C)-C(5)-C(5B)	109.1(5)	C(1D)-C(1)-C(1A)	69.2(4)
C(5C)-C(5)-C(5A)	109.1(4)	C(1E)-C(1)-C(1A)	136.1(8)
C(5B)-C(5)-C(5A)	110.6(5)	C(1F)-C(1)-C(1A)	42.4(4)
C(5C)-C(5)-C(4)	109.3(5)	C(1B)-C(1)-C(1A)	109.9(3)
C(5B)-C(5)-C(4)	109.4(4)	N(1)-C(1)-C(1C)	102.8(5)
C(5A)-C(5)-C(4)	109.4(5)	C(1D)-C(1)-C(1C)	41.6(4)
N(1)-C(1)-C(1D)	109.8(7)	C(1E)-C(1)-C(1C)	74.0(5)
N(1)-C(1)-C(1E)	106.0(6)	C(1F)-C(1)-C(1C)	143.8(7)
C(1D)-C(1)-C(1E)	110.8(3)	C(1B)-C(1)-C(1C)	109.2(3)
N(1)-C(1)-C(1F)	110.0(6)	C(1A)-C(1)-C(1C)	109.1(3)
C(1D)-C(1)-C(1F)	110.2(3)		

Table 4. Anisotropic displacement parameters ($\text{Å}^2 \text{x } 10^3$) for bott71a.
The anisotropic displacement factor exponent takes the
form: $-2\pi^2[\text{ h}^2\text{ a*}^2\text{U}^{11} + ... + 2\text{ h k a* b* U}^{12}]$

	U^{11}	U^{22}	U^{33}	U^{23}	U^{13}	U^{12}
N(1)	40(3)	32(4)	20(3)	-2(3)	5(2)	-8(2)
N(2)	40(3)	31(4)	19(3)	-1(3)	9(2)	0(2)
N(3)	38(2)	39(4)	13(3)	4(3)	1(2)	-6(3)
C(4)	24(3)	46(5)	23(4)	-6(3)	11(3)	1(3)
O(4)	45(2)	49(3)	7(2)	2(2)	-1(2)	-4(2)
C(5)	30(3)	48(5)	10(3)	-3(3)	6(2)	-2(3)
C(5A)	31(3)	42(5)	23(4)	4(3)	9(2)	0(3)
C(5B)	49(3)	42(5)	28(4)	-3(3)	19(3)	-1(3)
C(5C)	52(3)	51(5)	19(4)	-3(3)	4(3)	-14(3)
C(1)	44(3)	27(4)	16(4)	-2(3)	6(3)	-3(3)
C(1A)	57(3)	40(4)	51(4)	2(4)	24(3)	-8(3)
C(1B)	57(3)	40(4)	51(4)	2(4)	24(3)	-8(3)
C(1C)	57(3)	40(4)	51(4)	2(4)	24(3)	-8(3)
C(1D)	57(3)	40(4)	51(4)	2(4)	24(3)	-8(3)
C(1E)	57(3)	40(4)	51(4)	2(4)	24(3)	-8(3)
C(1F)	57(3)	40(4)	51(4)	2(4)	24(3)	-8(3)

Table 5. Hydrogen coordinates (x 10^4) and isotropic displacement parameters (Å^2x 10^3) for bott71a.

	x	y	z	U(eq)
H(3A)	-288	2364	6948	37
H(5AA)	4999	2551	6941	48
H(5AB)	4778	3304	6418	48
H(5AC)	2569	2814	5955	48
H(5BA)	1678	4048	7312	57
H(5BB)	471	3738	8475	57
H(5BC)	-208	3462	6897	57
H(5CA)	6411	3105	9386	62
H(5CB)	4605	3571	9944	62
H(5CC)	5751	3820	8704	62
H(1AA)	-1794	714	9807	71
H(1AB)	-4178	296	9280	71
H(1AC)	-4288	1086	9360	71
H(1BA)	4	216	7937	71
H(1BB)	-1525	198	6345	71
H(1BC)	-2311	-238	7520	71
H(1CA)	-5401	772	5670	71
H(1CB)	-6542	1081	6861	71
H(1CC)	-6287	296	6746	71
H(1DA)	-5758	939	8670	71
H(1DB)	-6547	433	7386	71
H(1DD)	-6376	1207	7086	71
H(1EA)	-1251	109	6667	71
H(1ED)	-3319	488	5579	71
H(1EB)	-3949	-107	6503	71
H(1FD)	0	676	9202	71
H(1FA)	-1635	33	9092	71
H(1FB)	-2310	690	9820	71